remote sensing

MDPI

Article

Study of Recent Deformations in the Bogotá Savanna and the City of Bogotá (Colombia) Using Multi-Temporal Satellite Radar Interferometry

Juan S. Tamayo Duque [1,2,*], Antonio Miguel Ruiz-Armenteros [1,3,4], Guillermo E. Ávila Álvarez [5], Gustavo Matiz [1,2] and Joaquim J. Sousa [6,7]

1 Department of Cartographic, Geodetic and Photogrammetry Engineering, Campus Las Lagunillas s/n, University of Jaén, 23071 Jaén, Spain; amruiz@ujaen.es (A.M.R.-A.); gmm00052@red.ujaen.es (G.M.)
2 Master Candidate, Geodetic Engineering and Applied Geophysics, Postgraduate Studies Centre, Campus Las Lagunillas s/n, University of Jaén, 23071 Jaén, Spain
3 Centre for Advanced Studies in Earth Sciences, Energy and Environment (CEACTEMA), Campus Las Lagunillas s/n, University of Jaén, 23071 Jaén, Spain
4 Research Group RNM–282 Microgeodesia Jaén, Campus Las Lagunillas s/n, University of Jaén, 23071 Jaén, Spain
5 Department of Civil and Agricultural Engineering, Faculty of Engineering, Universidad Nacional de Colombia, Ciudad Universitaria, Bogotá 111321, Colombia; geavilaa@unal.edu.co
6 Engineering Department, School of Science and Technology, University of Trás-os-Montes e Alto Douro, 5000-801 Vila Real, Portugal; jjsousa@utad.pt
7 Institute for Systems and Computer Engineering, Technology and Science INESC–TEC, 4200-465 Porto, Portugal
* Correspondence: jstd0001@red.ujaen.es

Abstract: Bogotá, the largest urban center and capital city of Colombia, is located within the Bogotá savanna, which originated as a lake in the central part of the Colombian Eastern Cordillera. Over time, the lake transformed into a gently undulating plain with horizontally deposited sediments that formed around five million years ago. Over the last few decades, the region has undergone significant population growth and rapid urban development, largely driven by migration from rural areas. This development has substantially impacted the subsidence observed in the city, primarily due to the extraction of groundwater. A previous study by the Servicio Geológico Colombiano (SGC) utilized data from GNSS stations and synthetic aperture radar interferometry (InSAR) with TerraSAR-X SAR between 2011 and 2017 to identify a subsidence pattern in the central region of Bogotá. The purpose of the study was to evaluate the risks and potential disasters associated with the subsidence phenomenon. Our study investigates both the subsidence in Bogotá, previously studied, as well as the rural savanna area, which is currently undergoing significant residential and industrial development. We utilized multi-temporal InSAR (MT-InSAR) techniques with Sentinel-1 SAR images from 2014 to 2021. The analysis results indicate that the outer regions of the city display the most significant subsidence, extending from the center to the north. The subsidence velocities in these areas reach approximately 5–6 cm/year.

Keywords: InSAR; subsidence; time series InSAR; PS–InSAR; Bogotá savanna; Bogotá DC; Sentinel–1

check for updates

Citation: Tamayo Duque, J.S.; Ruiz-Armenteros, A.M.; Ávila Álvarez, G.E.; Matiz, G.; Sousa, J.J. Study of Recent Deformations in the Bogotá Savanna and the City of Bogotá (Colombia) Using Multi-Temporal Satellite Radar Interferometry. *Remote Sens.* **2023**, *15*, 5249. https://doi.org/10.3390/rs15215249

Academic Editors: Thomas Oommen and Mirko Francioni

Received: 4 September 2023
Revised: 24 October 2023
Accepted: 31 October 2023
Published: 5 November 2023

Copyright: © 2023 by the authors. Licensee MDPI, Basel, Switzerland. This article is an open access article distributed under the terms and conditions of the Creative Commons Attribution (CC BY) license (https://creativecommons.org/licenses/by/4.0/).

1. Introduction

Land subsidence is a noteworthy environmental concern attributed to the extensive use of groundwater, mainly prevalent in arid and semi-arid regions. It affects the balance of underground water recharge and runoff, leading to the sinking of the land, which causes an array of problems including structural collapses and damage to transportation and energy networks [1]. The term "land subsidence" refers to either the gradual or abrupt sinking of the Earth's surface due to the movement of subsurface materials [2]. While subsidence

is generally a gradual process, certain human activities, including underground mining, intensive exploitation of aquifers, lowering of water tables, and extraction/expulsion of oil or gas, can hasten it. Other contributing factors include the consolidation processes of soft and organic soils [3].

Land subsidence has been observed in several countries and major cities worldwide. Examples of urban areas experiencing land subsidence due to groundwater extraction include Mexico [4], the San Joaquin Valley in California [2,5], Shanghai in China [6,7], Tokyo in Japan [8], Málaga and Guadalentín Basin in Spain [9,10], and Bologna in Italy [11]. Groundwater extraction is the main cause of subsidence in highly developed areas with complex geology, such as basins filled with unconsolidated alluvial, lacustrine, or shallow marine deposits, resulting in significant consequences such as land subsidence or settlement [12].

The damaging consequences of subsidence are apparent in a recent study regarding land subsidence resulting from the over-exploitation of groundwater in tectonic valleys in central Mexico [4]. The study presents instances of cities located in these valleys that have undergone differential ground subsidence since the 1980s, resulting in adverse effects on civil structures. The primary triggering mechanism is attributed to extensive groundwater extraction due to population growth as people migrate from rural to urban areas [13]. Groundwater extraction has a significant impact on urban centers. The study utilized interferometric synthetic aperture radar (InSAR) at different scales and during various time periods as it is a frequently utilized method of monitoring and measuring vertical and horizontal ground displacement in Mexico [4].

To investigate natural hazards resulting from human activity, different techniques are available, such as geodesy. The Global Navigation Satellite System (GNSS) and InSAR are commonly utilized geodetic techniques for the analysis of local deformations and spatiotemporal changes in the Earth's lithosphere [14]; or, as demonstrated in previous investigations [15–18], GNSS data have been used for the construction of models or analysis of deformations within the Earth's crust. Satellite radar interferometry, such as InSAR, provides the advantage of simultaneous analysis of large areas, resulting in extensive spatial coverage.

Several researchers in Colombia have studied subsidence in various regions of the country using a range of techniques, including topographic, geotechnical, and geodetic methods. During the 1990s, the Servicio Geológico Colombiano (SGC), previously known as INGEOMINAS, conducted subsidence studies in Bogotá, focusing on the city's seismic microzoning. The studies provided valuable soil information, including the characterization of clay deposits at different depths, as well as measurements of groundwater pressure through a network of piezometers. In May 2008, a comprehensive study was conducted to quantitatively assess elevation changes in Bogotá's geodetic network between 2003 and 2007, utilizing leveling network and GNSS data [19]. The analysis revealed differences between 0 and 31 mm between the two methods. Despite the methodological differences, both approaches confirmed the presence of active ground subsidence in the analyzed areas during that period. This highlighted the need for further monitoring campaigns and preventive measures. Consequently, the Fondo para la Prevención y Atención de Emergencias de Bogotá (FOPAE), in collaboration with the Institut Cartogràfic de Catalunya (ICC), conducted a differential InSAR (DInSAR) study to assess the evolution of ground subsidence in Bogotá from 1997 to 2009. The research revealed a subsidence map that highlighted a linear deformation rate of −75 mm/yr in certain neighborhoods of the city. Nevertheless, the study stresses the significance of using this method in neighboring rural areas to obtain reliable outcomes [20].

A comprehensive field study was conducted in 2011 to evaluate sites experiencing significant subsidence, as mentioned in the FOPAE and ICC study. The study consisted of updating previously installed piezometer readings and implementing numerical modeling techniques. The study's results indicated that the region with the most pronounced subsidence aligned with areas with high rates of groundwater extraction. A clear correlation was

observed between the accumulated subsidence and the cumulative volume of extracted water. On-site observations did not reveal any significant damage to buildings or local land deformations. However, it was postulated that this lack of significant impact could be attributed to the relatively modest differential settlements, which were insufficient to cause structural damage. The study concluded that a general subsidence phenomenon was occurring [21].

In 2020, a study was conducted using TerraSAR–X radar images to investigate the evolution of subsidence and quantify ground deformation in Bogotá from 2011 to 2017. The results revealed deformation values of −33 mm/yr, which were validated using GNSS data. These results offer convincing proof of the ongoing subsidence phenomenon in Bogotá. The consistency of the findings obtained from two independent geodetic methods [22] further supports this finding.

Our study applies multi-temporal InSAR (MT-InSAR) to investigate ground motion in the Bogotá savanna region, an area that has not been previously studied, as well as in the city of Bogotá. For that, Sentinel-1A/B SAR images were acquired in both ascending and descending orbits from 2014 to 2021. The primary goal of the study is to evaluate the evolution of subsidence patterns over time. To validate MT-InSAR processing outcomes for Bogotá city, we conducted a comparative analysis using data obtained from three GNSS stations: BOGT, BOGA, and ABCC. These stations are available on the Geodetic Reference System for South America (SIRGAS) website. The east and up components were analyzed, confirming the ongoing evolution of subsidence in the capital city. This evolution is supported by two distinct geodetic techniques. It is crucial, however, to implement additional geotechnical instruments to determine the underlying causes of subsidence in the city. Moreover, our study highlights the pressing need for executing a comprehensive management strategy aimed at guaranteeing the sustainable extraction of water from aquifers throughout the savanna region. While several studies suggest that the depletion of groundwater triggers subsidence, the absence of recent data throughout the entire savanna region emphasizes the need for establishing enhanced monitoring systems to identify the specific mechanisms causing subsidence.

2. Study Region

2.1. Bogotá Savanna

2.1.1. Geology of the Bogotá Savanna

The research site is situated in the Andean region of Colombia, specifically within the Cundinamarca Department's Bogotá savanna along the central axis of the Eastern Cordillera of Colombia, as illustrated in Figure 1. The area was once a lacustrine plain and has undergone minor dissection, with an altitude of 2600 m above sea level, as detailed in [23].

In the past, the savanna area was a lake that covered 157,000 ha in the Eastern Cordillera of the Colombian Andes [23]. Over time, sediment deposition from the Pliocene, Pleistocene, and upper Holocene periods gradually filled the lake. The sediment is primarily composed of horizontal lacustrine, fluvial, and fluvioglacial clay layers, with occasional thin silt, sand, and gravel layers, as well as multiple beds [24]. The Bogotá savanna is situated in the Upper Hydrographic Basin of the Bogotá River and can be segmented into two physiographic regions: the high plateau and the mountainous zone of the Eastern Cordillera. INGEOMINAS conducted a geological unit revision in the savanna area in 2005, which involved the identification and differentiation of regional structures within the rock formations. In the general description (Figure 1d, [25]), the following units were identified:

- Sabana Formation: Lacustrine deposits that emerge in the flat area made up mainly of clay and towards the margins of the organic, sandy clays and peat. It is in this deposit where the subsidence occurs.
- Bogotá Formation: A sequence of thick banks of sandstones and claystones.
- Cacho Formation: Conformed by grainy sandstones with some clay banks.
- Guaduas Formation: Clay–sandy sequence with coal seams.

- Labor-Tierna Formation: Very thick layers of sandstone interbedded with very thin layers of claystone.
- Plaeners Formation: Conformed by claystones, lydites, siltstones, and, to a lesser extent, very-fine-grained sandstones.
- Dura Sandstone: This unit is recognized by forming an abrupt morphology, derived from the lithology that is constituted mainly of sandstones with thicknesses up to 450 m.
- Chipaque Formation: It is made up of pyrite schists with intercalations of lime sandstone, loose sandstone, and lime levels.

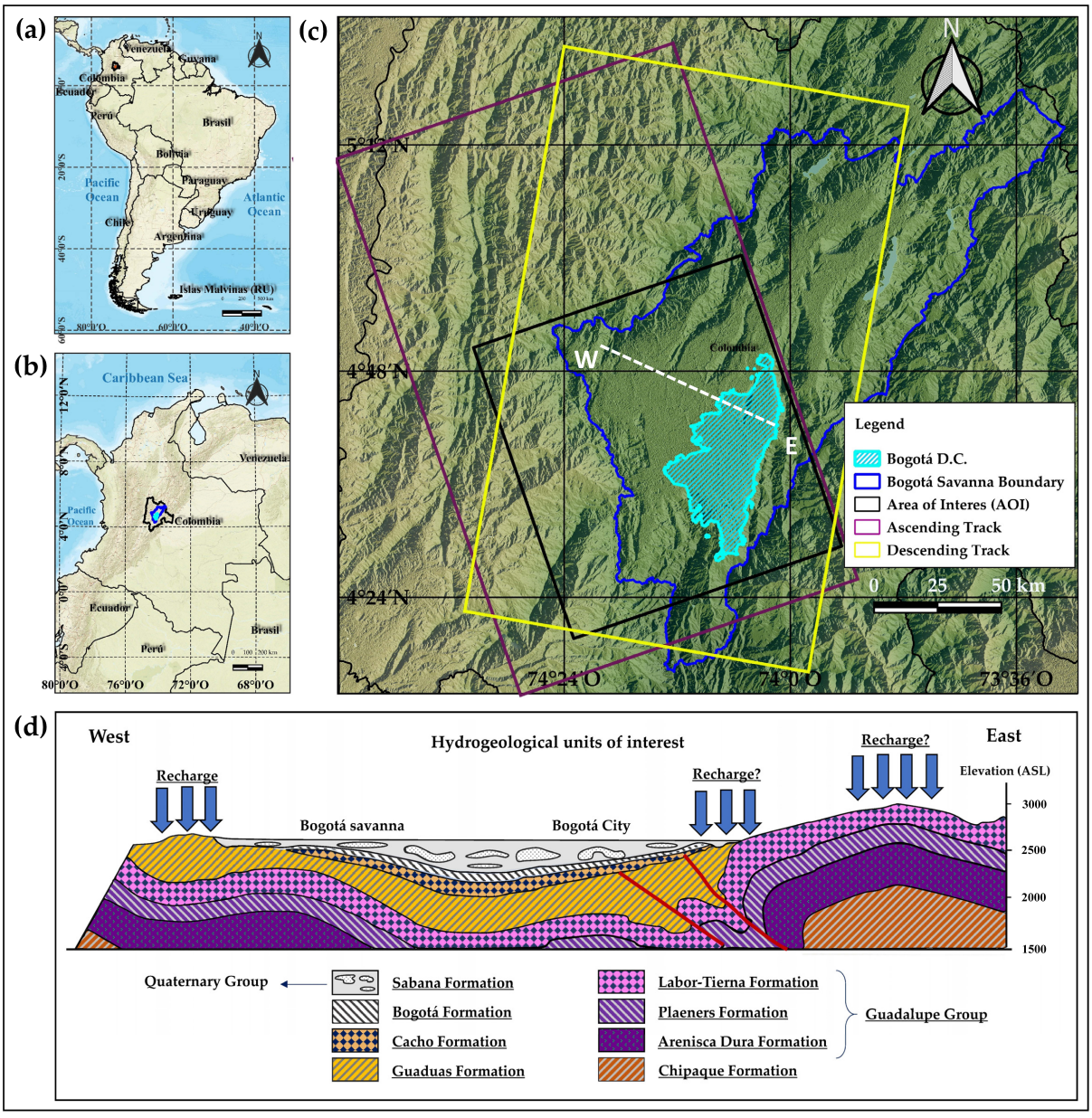


Figure 1. Location of the Bogotá Savanna: (**a**) Colombia's location in South America.; (**b**) the Cundinamarca Department is located in the center of the Eastern Cordillera, where the Bogotá Savanna can be found; (**c**) the Area of Interest (AOI) and footprints of the ascending and descending Sentinel-1 tracks utilized in this research are shown; (**d**) simplified hydrogeological profile for subsidence analysis; the section of this profile is indicated in panel (**c**) with a dashed white line (adapted from [21]).

The savanna plain of Bogotá covers one-sixth of the plateau's surface and includes the country's capital. The clay soils present in the northern and eastern parts of the area, as well as on the outskirts of the city, contribute to soil degradation and shrinkage. Due to the study area's complex topography and geological features, it presents an outstanding opportunity to explore the effect of clay soils on the environment and its residents [26].

2.1.2. Hydrogeology of the Bogotá Savanna

Access to underground water in the Bogotá savanna is crucial for providing drinking water to diverse populations, supporting agriculture, and sustaining industries. Accordingly, there has been a marked rise in drilling wells at greater depths due to the insufficiency of surface water resources to satisfy the escalating demand [27]. In the savanna, land subsidence has been linked by various authors and government agencies to groundwater extraction from shallow aquifers and population growth. One factor contributing to this growth is the migration of people from the capital district to peripheral municipalities, motivated by lower living costs, improved housing options, and better living conditions compared to larger cities [28]. In recent years, the growth of large, medium, and small companies within the savanna has contributed to an increase in population due to high costs in the capital city and tax reductions for free zones.

The rainy seasons in the Bogotá savanna are crucial as they aid in recharging the region's aquifers, which are necessary for maintaining the water table. The decrease in mean river currents is linked to elevated temperatures during the summer and hydroclimatic anomalies [29].

The Bogotá savanna's critical area has been the subject of numerous hydrogeological surveys, with the purpose of evaluating sustainable groundwater management and exploitation. The "Plan de Manejo Ambiental de Aguas Subterráneas en la Sabana de Bogotá y zona critica" study was conducted by INGEOMINAS (now SGC) and the Corporación Autónoma Regional de Cundinamarca (CAR) in the region. The study analyzed the geology, hydrogeology, and hydrochemistry of nine sub-basins within the upper and middle basins of the Bogotá River. The study's findings provide insights into the consequences of withdrawing groundwater [30]. The study revealed a decrease in the region's hydrogeological potential due to economic development and population growth in the Bogotá savanna. The hydrogeological sub-basins that were examined in this study are presented in Table 1 and Figure 2a.

Between 1997 and 2006, CAR conducted a groundwater-level measurement campaign in various wells and water tanks located in the savanna to determine the total average flow extracted from each aquifer underlying the hydrogeological sub–basins listed in Table 1. Table 2 shows the main affected aquifers for each sub–basin in the region and the fluctuation of the water table.

Based on the analysis conducted by CAR [30], different industries and population groups primarily extract groundwater from the Quaternary and Guadalupe formations in the Bogotá savanna region. Furthermore, critical areas were identified by analyzing the decrease in the water table level in aquifers due to water extraction in each of the hydrogeological sub-basins (see Table 2). In some urban areas of municipalities in the Bogotá savanna, there is significant variation in the water table levels, ranging from 1 to 28 m. The municipalities of El Rosal, Funza, Chia, Cajicá, and Madrid, as well as the Guaymaral sector to the north of the municipalities of Bogotá, are notable examples of these areas with significant declines.

During periods of normal rainfall, groundwater extraction operations running less than 10 h per day record flows in the order of 7,030,000 m^3. However, during episodes of drought or El Niño occurrences, the need for groundwater extraction surges to levels ranging between 28,000,000 and 35,000,000 m^3, with the exception of the metropolitan area [30].

Table 1. Sub-basins defined for assessing potential groundwater reduction.

No.	I	II	III	IV	V	VI	VII	VIII	IX
Sub–basins	Sisga	Tominé	Teusacá	Neusa	Fontibón	Chicú	Subachoque	Basillas	Tunjuelito

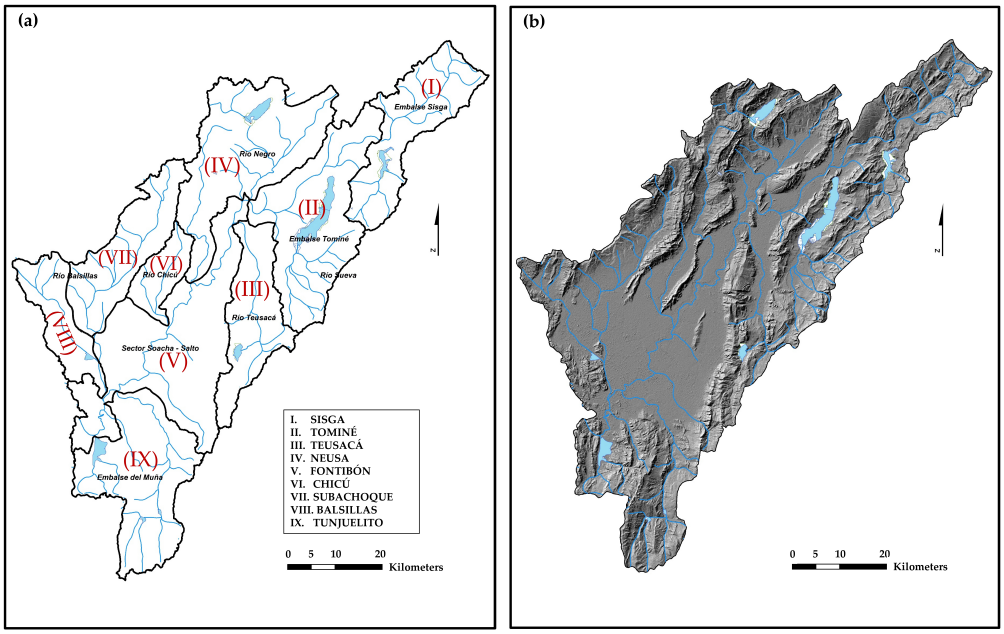


Figure 2. (**a**) Hydrogeological sub-basins of the Bogotá savanna studied by INGEOMINAS (SGC) in 1989. The region was analyzed and divided into nine hydrogeological sub-basins, which were integrated into the Upper and Middle Basins of the Bogotá River. The source for this information is Corporación Autónoma Regional de Cundinamarca (CAR) [30]. (**b**) Relief of the Bogotá savanna (adapted from [30]).

Table 2. Progressive decrease in piezometric levels in hydrogeological sub-basins from 1997 to 2006 as classified by CAR [30].

No.	Sub–Basin	Aquifer Related	Fluctuation Analysis Static Level
I	Sisga	Paleogene Cretaceous Guadalupe	*
		Quaternary Neogene	<5 m
II	Tominé	Paleogene Cretaceous Guadalupe	*
		Quaternary Neogene	Declines of 5 m
III	Teusacá	Paleogene Cretaceous Guadalupe	*
		Quaternary Neogene	Gradual Declines between 5 and 10 m
IV	Neusa	Paleogene Cretaceous Guadalupe	Declines between 1 and 10 m
		Quaternary Neogene	Declines of 10 m
V	Fontibón	Paleogene cretaceous Guadalupe	*
		Quaternary Neogene	Declines between 5 and 15 m
VI	Chicú	Paleogene Cretaceous Guadalupe	Declines between 15 and 50 m
		Quaternary Neogene	Declines between 5 and 25 m
VII	Subachoque	Paleogene Cretaceous Guadalupe	*
		Quaternary Neogene	Declines between 10 and 30 m
VIII	Basillas	Paleogene Cretaceous Guadalupe	*
		Quaternary Neogene	Declines between 5 and 15 m
IX	Tunjuelito	Paleogene Cretaceous Guadalupe	*
		Quaternary Neogene	Declines between 5 and 15 m

(*) Non–Data collected, insufficient information.

The study conducted by CAR illustrates the notable decline in the Quaternary and Guadalupe aquifers depending on their location during the season, ultimately leading to groundwater depletion. It was discovered that in critical areas of Bogotá savanna where wells are situated, during seasons with intense heat, the natural recharge of these aquifers is insufficient, causing a reduction in underground water potential [30]. Land subsidence can result from various factors, but the largest contributor in the region is deep groundwater withdrawal [21]. To address this problem, the only feasible solution is to achieve a balance between the amount of water pumped from aquifers and the amount recharged through natural processes such as rainwater filtration (climate) or by pumping recycled water into the soil [31].

2.2. Bogotá D.C.

2.2.1. Geology of Bogotá

The capital of Colombia, Bogotá, is located in the largest province of the region, the Bogotá savanna. Most of its inhabitants live at an altitude of approximately 2600 m above sea level, on lake deposits that are primarily situated beneath the city. The city is encircled by high mountains belonging to the Eastern Andes and forms a basin. Urbanization has taken place along the mountain slopes from south to north. The high relief areas comprise fractured sedimentary rocks covered by thick colluvium, alluvium, sands, and gravels of fluvial terraces, fluvioglacial, and fan deposits [32]. Geologically, Bogotá is located on a vast sedimentary fill, which constitutes the Bogotá savanna and is ringed by hills made up of sandstone-type rocks, claystone, and conglomerates [33].

2.2.2. Hydrogeology of Bogotá

The hydrological characteristics of Bogotá are similar to those described in the Bogotá savanna section, due to its location within the savanna.

Based on statistical data from the Departamento Administrativo Nacional de Estadística (DANE), Bogotá's estimated population in 2021 was 7,834,167 residents. The migration to the interior of the country has affected living standards in many towns and municipalities [34].

As reported in [34], the city's population has increased by a factor of 8.5 over the last 60 years, from 883,410 residents in 1952 to 7.47 million inhabitants in 2011. This growth creates pressure on land use and the environment. The expansion of local residential communities has impacted rural properties. Moreover, the construction plan for the industrial zone raises concerns about potential future contamination problems and indiscriminate depletion of natural resources [35]. An increase in water consumption in both the industrial and residential sectors of the city can be observed, which is attributed to population growth. Data from 2020, supplied by the Bogotá Aqueduct and Sewerage Company (EAAB), categorized water consumption by use type. Residential consumption, linked to the number of households and individuals, amounted to a daily total of 650,774,904 L. On the other hand, the non-residential sector reported a daily demand of 37,164,547 L. [36].

This increased water consumption has various implications, including its impact on the local environment, as demonstrated by Ávila [37], particularly in relation to the shrinkage and cracking phenomena of clay soils in Bogotá. The study conducted various geotechnical tests on samples from a lake deposit to simulate conditions that can lead to these phenomena. Groundwater extraction was identified as the main cause of subsidence cracks that lead to soil desiccation. However, deep geological structures such as faults or lithological contacts can cause surface discontinuities, steps, and cracks in subsidence-prone areas. Non-uniform deformations may also occur due to these structures, leading to such surface irregularities.

Moreover, there are other contributing factors apart from groundwater extraction's connection to subsidence. These factors consist of (a) a reduction in piezometric levels in deeper layers of the ground; (b) drying of the surface as a result of lower groundwater levels; (c) the impact of vegetation; (d) the weight exerted on the ground from widespread

construction; (e) ground surface lowering caused by tectonic effects related to the regional arrangement of tectonic plates; (f) secondary consolidation of clay deposits caused by viscous effects without load level changes; and (g) subterranean works and deep mining operations [21].

3. Data and Methods

3.1. InSAR and GNSS Data

This study analyzed the Bogotá savanna and Bogotá city through Sentinel-1A/B SAR images in the C-band spectrum, with a wavelength of approximately 5.7 cm and a frequency of 5.3 GHz. For the analysis, single-look complex (SLC) images were obtained from the interferometric wide (IW) swath mode, providing a wide coverage of the area with image dimensions of 240 × 170 km. The study specifically used images with vertical polarization (VV). Two independent datasets were utilized for this study, acquired from different geometries, including ascending and descending orbits. The ascending dataset comprises 107 SAR scenes captured between October 2014 and May 2021, located in the middle of sub-swath 2. Likewise, the descending dataset includes 153 SAR scenes captured between October 2014 and May 2021, also located in the middle of sub-swath 2. Table 3 provides the main characteristics of these two datasets. The distribution of temporal and perpendicular baselines utilized in the MT-InSAR analysis for both ascending and descending datasets is displayed later in Section 3.2.1.

Table 3. Sentinel-1A/B C-band SAR data used in this study (wavelength of 5.7 cm).

Parameter	Ascending	Descending	Acquisition Mode
Acquisition period	15 October 2014–29 May 2021	10 October 2014–24 May 2021	
Total Number of Scenes in period	107	153	
Track Number	150	69	Interferometric
Look Angle (°)	39.33°	39.56°	Wide (IW)
Heading Azimuth (°)	348.33°	191.65°	
Number of PS Points Generated	263,669	284,778	

As a secondary verification method, we utilized time series data from three GNSS stations (BOGT, BOGA, and ABCC) located in Bogotá city, as illustrated in Figure 3. Subsidence in areas where antennae are installed has been recorded over the last few decades at these stations, as demonstrated by multiple studies. BOGT is located in a green space within the SGC building, while BOGA is situated on the rooftop of the Agustín Codazzi Geographic Institute (IGAC) [22], and ABCC is situated at the "Empresa de Acueducto y Alcantarillado de Bogotá" (EAAB). These stations are all included in the MAGNA-ECO, which is Colombia's nationwide Continuous Operation GNSS Station Network. The information gathered by these stations is transmitted to different SIRGAS processing centers located in South America. Subsequently, the data are processed to acquire final solutions that are openly published by the official organization of SIRGAS. The primary purpose is to examine the fluctuations in eastern and upward components throughout the study duration and to verify if the deformation rates align with the results of the time series analyzed in the MT-InSAR study. The BOGT and BOGA stations have been in operation since 2000, providing a dataset that covers about 21 years until 2021. On the other hand, the ABCC station joined the SIRGAS network in 2010, resulting in a dataset that spans a period of 11 years.

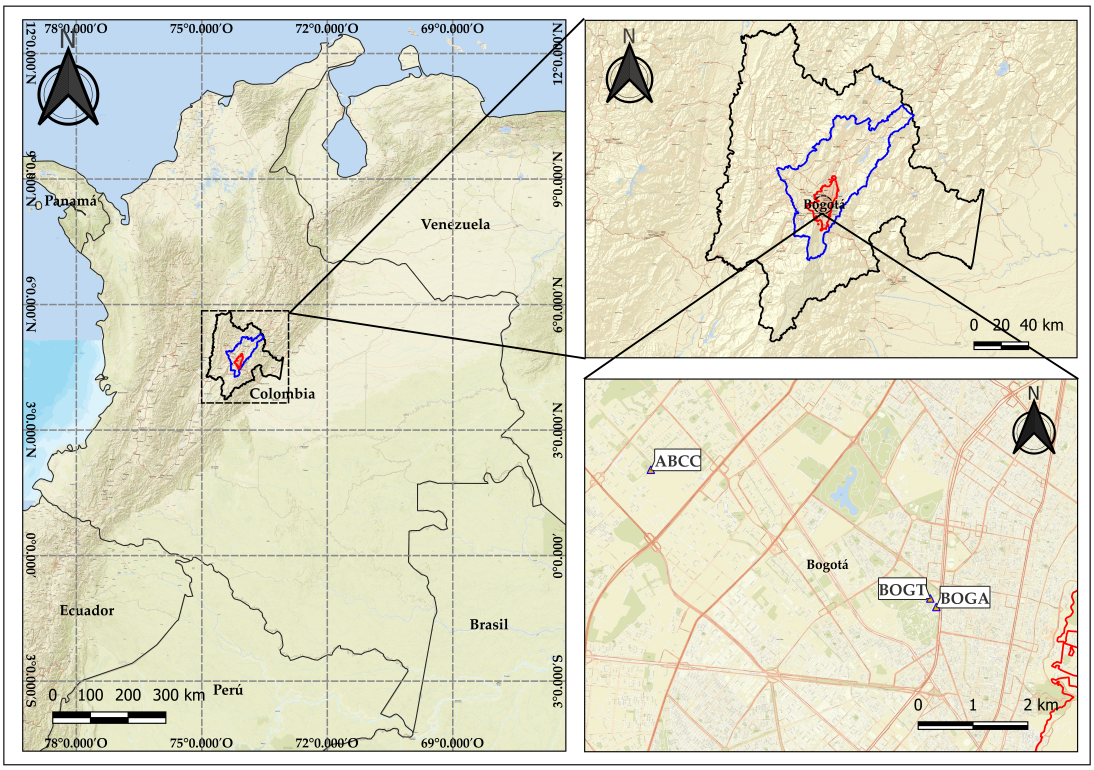


Figure 3. Location of GNSS stations BOGT, BOGA, and ABCC in Bogotá.

3.2. Methods

This study uses modern space-geodetic techniques to measure surface deformation, particularly subsidence, in the Bogotá savanna and Bogotá city. Advanced MT-InSAR methodology [38] was employed to analyze the vertical surface displacement within the Area of Interest (AOI) of the savanna. Furthermore, data from GNSS stations processed by SIRGAS have been incorporated. These advanced techniques enable us to precisely detect and analyze a variety of surface changes, including changes in topography, roughness, and both horizontal and vertical displacements.

3.2.1. Synthetic Aperture Radar Interferometry

InSAR is a valuable tool for measuring the surface deformation of the Earth and analyzing changes in its characteristics independent of weather conditions. It is widely employed in monitoring and assessing risks connected to volcanic, seismic, landslide, and hydrogeological processes, as well as human activities such as mining, fluid extraction, and injection [39]. Radar technology adopts a coherent approach to produce interferograms that result from combining an image with its complex conjugate. When corresponding pixels in both images show correlation, the interferometric phase provides highly accurate measurements of the distance between the sensor and the object [40]. This phase accurately represents the alignment between the two radar signals and constitutes a portion of the wavelength. Because microwave signals have a wavelength on the order of centimeters, the interferometric phase has the potential to detect distance changes with sub-millimeter precision [40].

However, InSAR technology is not without constraints. Terrain reflectivity can trigger radar decorrelation, leading to difficulties in interpreting the InSAR phase. Moreover, atmospheric water vapor can introduce delays in the radar signal, resulting in precise but not accurate phase measurements. It took more than a decade to tackle these limitations by developing methods that leverage multi-temporal data, as reported in [40].

In recent years, several challenges linked to long-term InSAR usage have emerged. These encompass interferogram decorrelation due to temporal and/or geometric changes,

interferometric phase unwrapping, and discerning residual topography from terrain displacement in uncertain target regions. Despite attempts to combat these issues, atmospheric effects can still compromise results and result in misinterpretation of detected signals [40].

To overcome temporal and geometric decorrelations in DInSAR, various MT–InSAR techniques have been developed [41–45]. In this study, we utilized one of these MT-InSAR techniques, specifically permanent/persistent scatterers InSAR (PS-InSAR), to primarily detect single coherent pixels within a set of multiple SAR images with a large baseline (even larger than the decorrelation). The permanent/persistent scatterers (PS) pixels [45] are isolated points with phase signatures. They can be consistently explained over time. Various methods have been developed to identify and isolate the PS pixels in the interferogram. The methods employ functional models to map deformation changes over time. They have successfully identified PS pixels in both urban and non-urban areas experiencing predominantly stationary or periodic deformations.

Radar image analysis was carried out with SARPROZ software (www.sarproz.com, accessed on 1 October 2023). The PS-InSAR results were obtained by following the workflow shown in Figure 4, which is briefly described below.

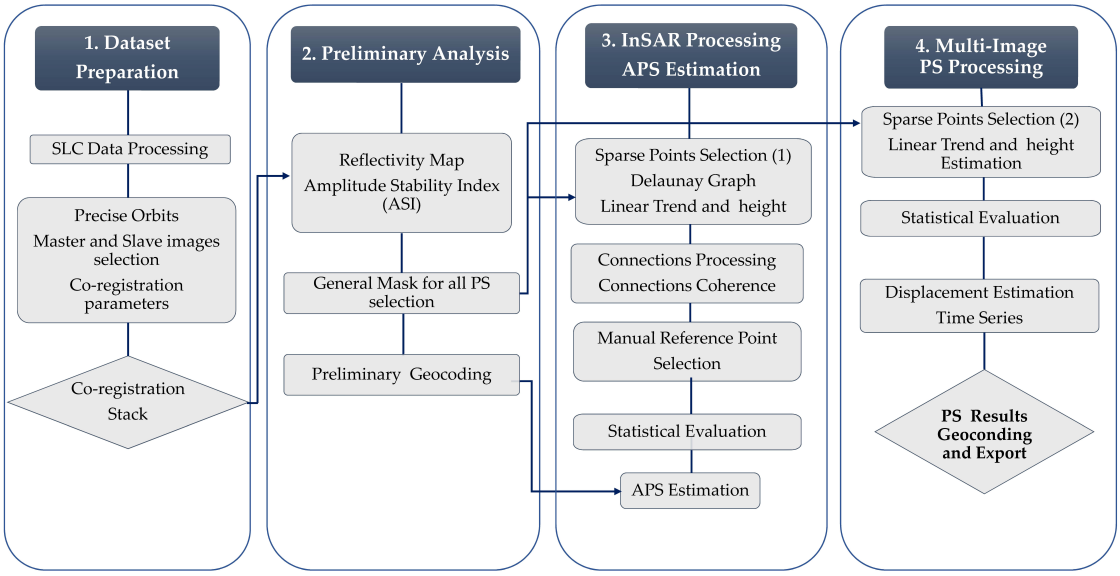


Figure 4. Workflow illustrating the simplified processing steps used in SARPROZ for PS–InSAR analysis.

The processing begins with image import, precise orbit application, and dataset definition, which includes the selection of master and slave images. Section 3.1 depicts that the initial stack consists of 107 images taken between 15 October 2014 and 29 May 2021 in the ascending orbit (as shown in Table 3). For this stack, the master image acquired on 2 June 2018 was selected. The second set comprises 153 images in a descending orbit obtained from 10 October 2014 to 24 May 2021, with the main image acquired on 26 February 2017 (see Table 3). Once the master image is selected and the slave images are extracted, co-registration is performed using precise orbits. Figure 5 depicts the temporal and perpendicular baseline distribution for both ascending and descending datasets.

The second step of the process entails conducting a preliminary analysis to calculate the reflectivity map and Amplitude Stability Index (ASI) for the entire AOI. Subsequently, a mask is chosen for point selection, and a preliminary geocoding is performed by utilizing the 1 arc-second Shuttle Radar Topography Mission (SRTM) Digital Elevation Model (DEM).

The next phase consists of InSAR processing, wherein interferograms, coherence of interferograms in the image space, and spatial coherence (average coherence of selected interferograms) are calculated. Initial multitemporal analysis involves estimating the

atmospheric phase screen (APS), which is then evaluated and eliminated for each SAR image using different filters [40,46]. The *ASI* was computed via Equation (1):

$$ASI = 1 - D_A = 1 - (\sigma_A / m_A), \quad (1)$$

where D_A represents the amplitude dispersion, σ_A represents the standard deviation of amplitude over time, and m_A represents the mean deviation of amplitude in time.

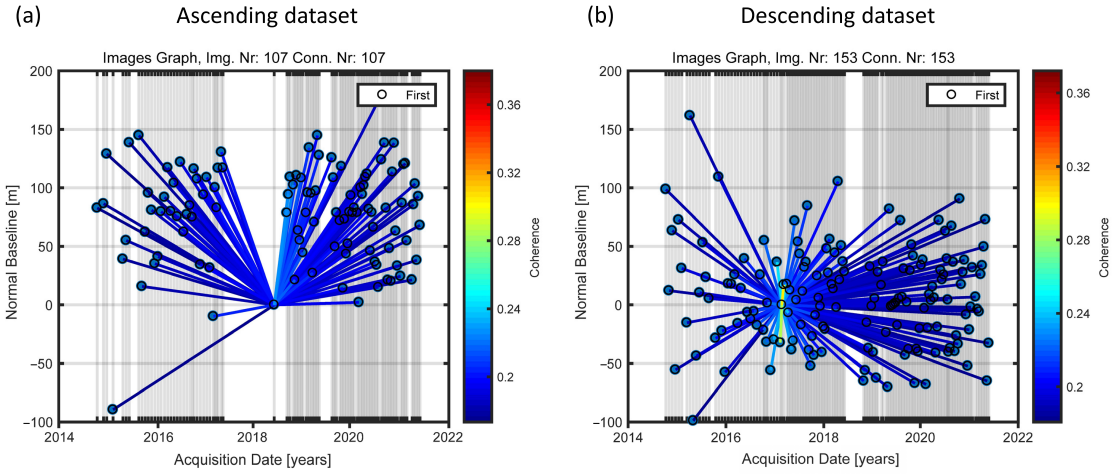


Figure 5. Temporal vs. perpendicular baseline distribution for the ascending (**a**) and descending (**b**) tracks. The color bar represents the average spatial coherence for all interferograms.

Prior to conducting a phase stability assessment, it is necessary to estimate and remove influences such as APS, DEM errors, and orbital inaccuracies. In contrast to phase, absolute amplitude values are less affected by these phenomena. Therefore, pixels that maintain similar amplitude across multiple data acquisitions are expected to have minimal phase dispersion [38].

In this study, an ASI threshold of greater than 0.75 was set for the initial selection of sparse points, which reduced the number of data points but improved the accuracy of APS estimations. The first PS points create a reference network through Delaunay triangulation, and calculations include differential deformation velocity and residual topographic error for each connection. A linear model of linear height residuals and displacement velocities is then subtracted, resulting in APS obtained from phase residuals by graph inversion. One PS is fixed as a reference, and APS quality is assessed by temporal coherence analysis after graph inversion and APS removal.

We select final PS points for subsequent estimations of linear velocity and height after APS estimation. To ensure dense PS point coverage, we applied a threshold of ASI greater than 0.6. For this multi-image PS processing, we utilized similar parameters and a reference point used during APS estimation. Deformations with respect to the reference point are shown in the line-of-sight (LOS) direction. Positive movements, which indicate PS moving towards the sensor, are displayed on deformation maps in blue; negative movements, indicating PS moving away from the sensor, are shown in red.

The final stage includes geocoding and visualization, generating temporal deformation series for PS points with temporal coherence greater than 0.6–0.7.

This processing was performed independently for both ascending and descending datasets. After obtaining LOS deformations for both orbits, vertical and east–west horizontal components for each PS are extracted through movement decomposition.

3.2.2. GNSS

In Colombia and South America, GNSS stations have been placed throughout the country as reference bases for differential surveys, receiving real-time satellite informa-

tion [47]. These stations have been installed by both the IGAC, which is responsible for the country's national geodetic reference systems, geographic investigations, and cadaster, and the SGC, which evaluates and monitors geological hazards nationwide. The Colombian stations in the active network conform to the country's official reference frame, MAGNA SIRGAS, ensuring high-quality and reliable spatial data generation. This conformity guarantees the alignment of Colombian coordinates with positioning space techniques and international georeferenced datasets [48]. The processing of coordinates for MAGNA-ECO stations involves collaborating with the regional analysis center of the International GPS Service (IGS-RNAAC-SIR, Regional Network Associate Analysis Center SIRGAS) to ensure that the coordinates remain continuously aligned within the coordinate system of GNSS satellites [48]. The network of GNSS stations across the continent is formed by Colombian stations, which are included in the Geodetic Reference System for the Americas (SIRGAS). These stations follow a consistent definition of the International Terrestrial Reference System (ITRS) and serve as a regional augmentation of the International Terrestrial Reference Frame (ITRF) in the Americas and the Caribbean. SIRGAS stations are classified into two primary categories: the continental network (SIRGAS-C) and several densification networks known as national reference networks (SIRGAS-N) [49]. The continental network comprises stations that are strategically located throughout Latin America, while the densification networks are specific to individual countries.

In South America, the SIRGAS processing centers produce weekly coordinates for their stations, with the involvement of at least three processing centers. These coordinates adhere to unified standards to ensure accurate calculations based on criteria set by the International Earth Rotation and Reference Systems Service (IERS) and specific guidelines for GNSS defined by the International GNSS Service (IGS). The solutions calculated by each center are combined to generate weekly solutions within the same IGS reference frame. The management of the continental SIRGAS-C network is conducted by the Deutsches Geodätisches Forschungsinstitut Technische Universität München (DGFI-TUM), which consolidates solutions provided by other centers into a single solution.

The DGFI-TUM conducted the processing of solutions for the BOGT, BOGA, and ABCC GNSS stations located in Bogotá, which belong to the Colombian active monitoring network MAGNA-ECO, and SIRGAS-C, under the supervision of Dr. Laura Sanchez and Hermann Drewes, both members of the SIRGAS scientific organization. The most recent update of the multi-annual solutions has been incorporated for all stations within the SIRGAS Reference Frame, considering the latest update of the International Terrestrial Reference Frame (ITRF 2020). Access to SIRGAS data is available on the official SIRGAS website (https://www.sirgas.org/en/stations/, accessed on 1 October 2023).

To update the solutions of the mentioned SIRGAS stations, the GNSS data were processed using Bernese GNSS software version 5.2, which included an analysis of discontinuities in station positions due to seismic offsets or antenna configurations. For more comprehensive information or for readers interested in delving deeper into the state-of-the-art GNSS data processing, refer to the SIRGAS publications in Latin America [50–52].

4. Results

4.1. Multi-Temporal InSAR

We utilized an MT-InSAR method to assess and process the Sentinel-1A/B datasets, examining the spatiotemporal accumulation of ground deformation in the LOS direction over the Bogotá savanna and the city of Bogotá during the study period. For this study, the hills of Suba were chosen as a reference (Figure 6), a region within the city characterized by the presence of hard, erosion-resistant sandstones, a type of rock known for its relatively stable geological properties compared to the clayey soils that predominate throughout the city [53]. The analysis included a total of 284,778 scatterers for the ascending track and 263,669 for the descending track. The scatterers were primarily concentrated in densely populated urban areas within the savanna, particularly the city of Bogotá, which provided the most representative individual results for the MT-InSAR analysis (Figure 6a,b).

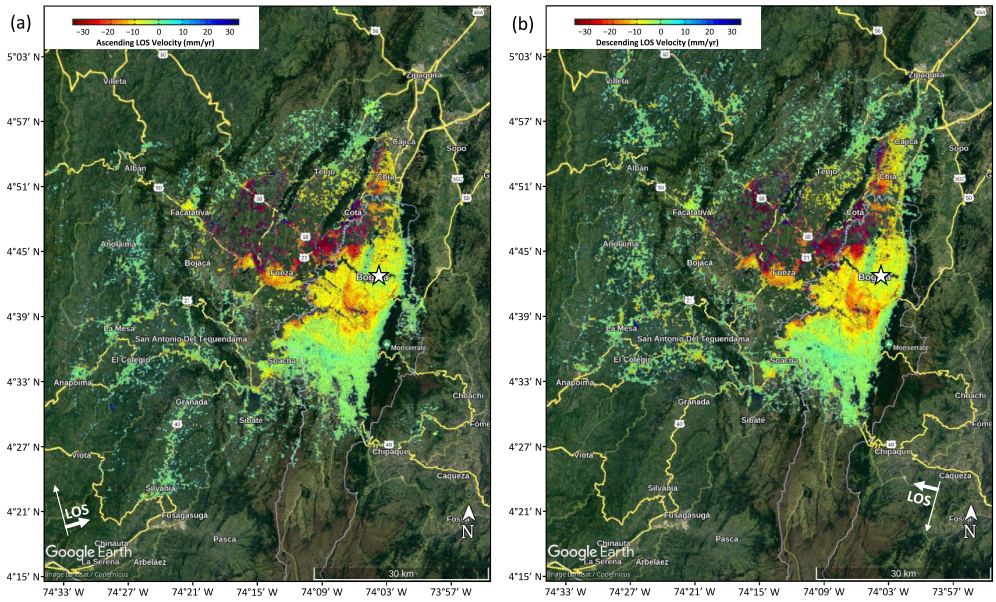


Figure 6. Mean LOS velocity (mm/yr) maps for the savanna and the city of Bogotá derived from this MT-InSAR analysis for the period 2014–2021. (**a**). Results for the ascending track. (**b**) Results for the descending track. The white star represents the area assumed to be stable for reference purposes.

The study found a regular vertical cumulative deformation pattern ranging from −100 to −400 mm in various municipaleities in the central and southwestern regions of the savanna. These include Madrid, Mosquera, Funza, Facatativá, Cota, El Rosal, Buenavista, and Chia, among others (see Figure 7a). Meanwhile, horizontal deformation rates varied primarily between 0 and 100 mm towards the east during the study period (see Figure 7b).

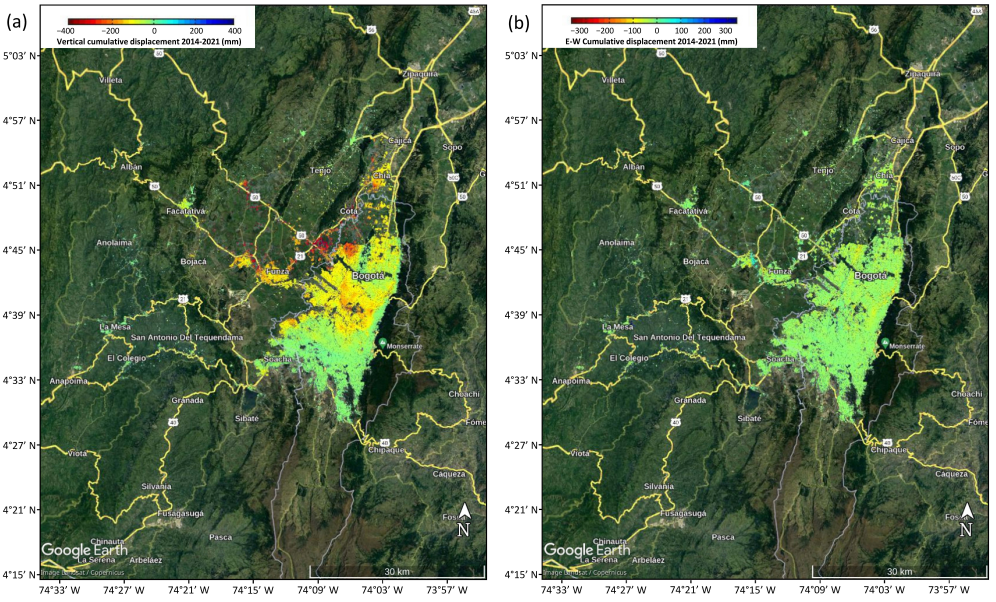


Figure 7. MT-InSAR processing results of the AOI. (**a**) Vertical cumulative displacement map. (**b**) East–west horizontal cumulative displacement map. The highlighted regions in red indicate rates of cumulative displacement between −200 mm and −400 mm during the period of 2014–2021. For the cumulative displacements in the east–west direction, red colors indicate movements towards the west, while blue colors indicate movements towards the east.

Figure 8a exhibits a vertical rate map of velocity, indicating subsidence that ranges from −30 to −40 mm/yr across multiple municipalities in the savanna, reaching up to

−50 to −60 mm/yr in some areas. Furthermore, Figure 8b highlights particular zones within the savanna region where eastward displacement, denoted by smaller blue dots, is observed with a velocity of approximately 15 mm/yr.

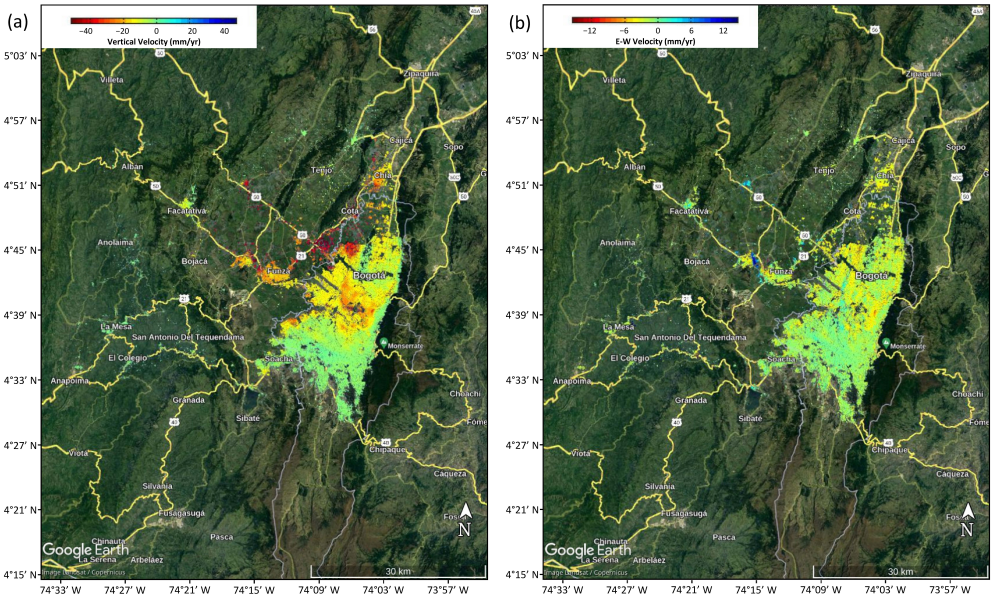


Figure 8. MT-InSAR deformation rates of the AOI. (**a**) Vertical velocity map and (**b**) east–west velocity map. The east–west velocity map denotes movements to the west with red color and movements to the east with blue color.

The MT-InSAR analysis demonstrates ground movements across the AOI in both tracks. Figure 9 identifies 16 specific areas where ground deformation is particularly significant.

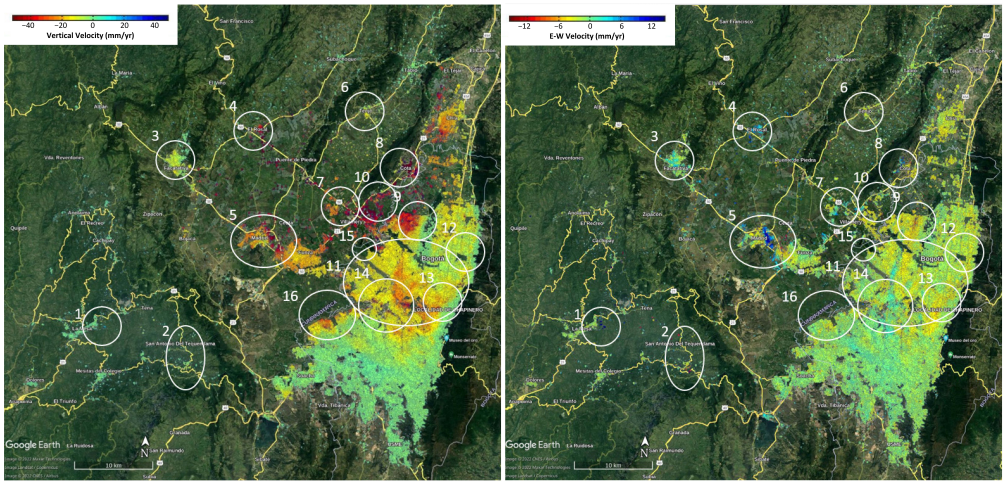


Figure 9. The MT-InSAR analysis performed in the Bogotá savanna and Bogotá city has produced vertical (**left** image) and east–west (**right** image) deformation velocity rates, as shown. White circles represent areas 1 through 16 that were chosen for a detailed analysis.

Zone 1, shown in Figure 10, corresponds to the La Mesa municipality located in the Bogotá savanna. The MT-InSAR analysis conducted in this area uncovered a slight uplift movement below 10 mm/yr and an eastward movement in a zone containing country houses.

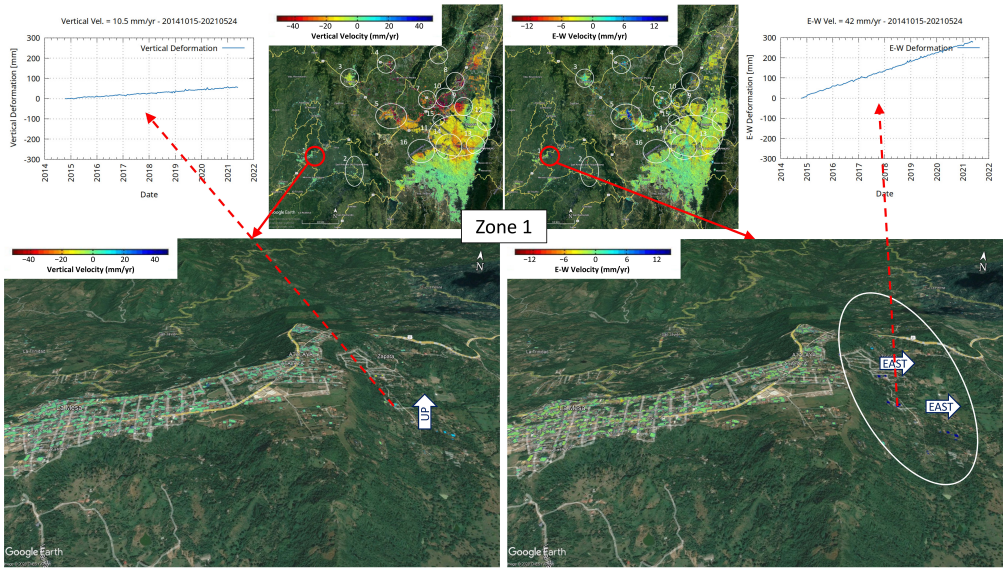


Figure 10. Time series results of the vertical and east–west deformation velocity rates for the municipality of La Mesa. The white ellipse indicates an area with eastward displacement.

Figure 11 identifies zone 2, which is located in the municipality of San Antonio de Tequendama, nearby the Bogotá savanna. Here, a westward slope displacement and vertical subsidence have been observed. Meanwhile, Figure 12 illustrates the observed area in zone 3, which corresponds to Facatativá municipality. The figure shows movements towards the east ranging from 0 to 6 mm/yr, alongside vertical subsidence ranging from 0 to −20 mm/yr. It is worth noting that the areas surrounding Facatativá, such as crop fields, greenhouses, and warehouses, have higher rates of subsidence in the vertical direction and eastward movements compared to those observed within the municipality itself.

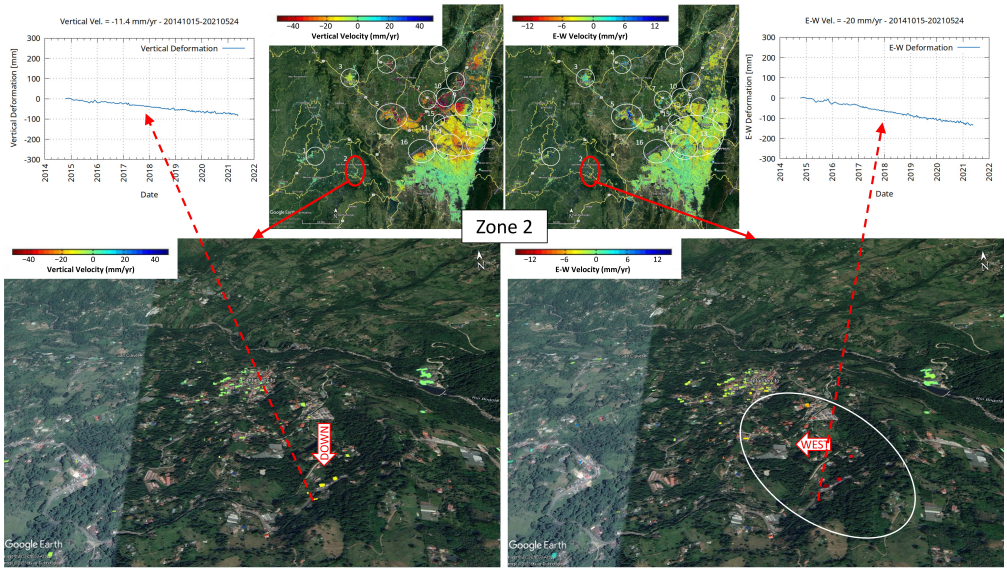


Figure 11. Time series results of the vertical and east–west deformation velocity rates for the municipality of San Antonio de Tequendama. The area marked with the white ellipse indicates a landslide to the west.

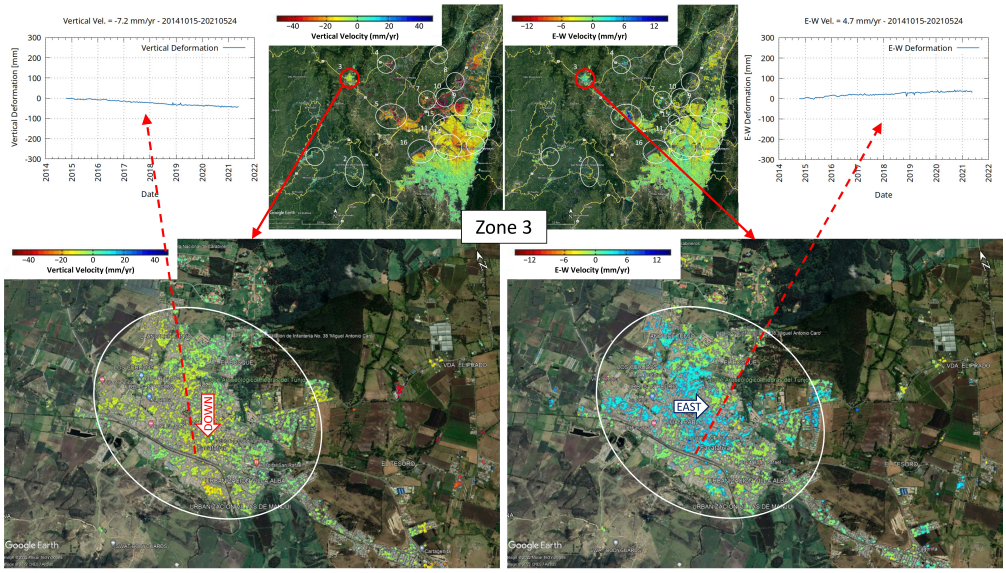


Figure 12. Time series results of the vertical and east–west deformation velocity rates for the municipality of Facatativá. In this area, a slight eastward movement with a vertical component of subsidence can be seen.

Figure 13 illustrates zone 4, which includes the municipality of El Rosal. The area is situated in a flat region surrounded by farmland and greenhouses and has a well-known subsidence issue caused by the declining piezometric level in the CAR study area. The root cause of this problem is groundwater extraction from the Quaternary and Guadalupe aquifers. The MT-InSAR analysis indicates a notable downward vertical movement ranging between −20 and −40 mm/yr across the municipality and its surroundings. Furthermore, an observed eastward movement of up to 6 mm/yr exists.

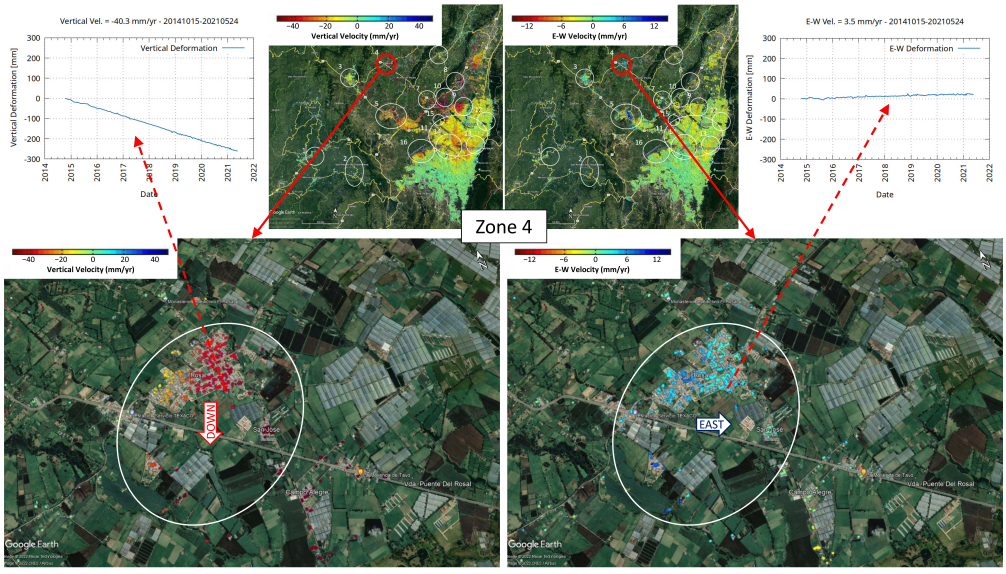


Figure 13. Time series results of the vertical and east–west deformation velocity rates for the municipality of El Rosal. The area marked with a white ellipse indicates a subsidence of the terrain with a slight eastward component.

Zone 5 corresponds to the Municipality of Madrid, as shown in Figure 14. This region is characterized by its proximity to a hill and the expansion of urban infrastructure into the surrounding flat area. Similar to zone 4, the municipality experiences subsidence due to the growth of industries and agricultural irrigation. The MT-InSAR data show vertical

displacements ranging from −20 to −40 mm/yr. Furthermore, a shear motion is detected, with deformation rates of 10 mm/yr towards the east and −6 mm/yr towards the west.

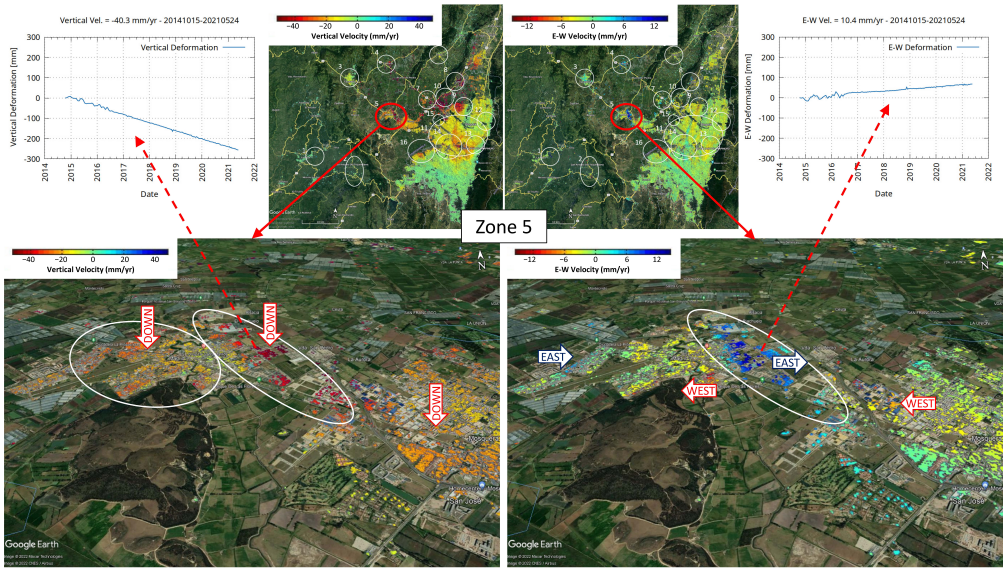


Figure 14. Time series results of the vertical and east–west deformation velocity rates for the municipality of Madrid. This zone shows two areas of subsidence and associated horizontal movement. The east-trending slope slide is the most prominent, marked by the white ellipse on the right.

Zone 6, shown in Figure 15, represents Tenjo Municipality at the foot of the mountain slope. In this district, the MT-InSAR analysis captures vertical displacements ranging roughly from −10 to −30 mm/yr, accompanied by westward displacements ranging from 0 to −6 mm/yr.

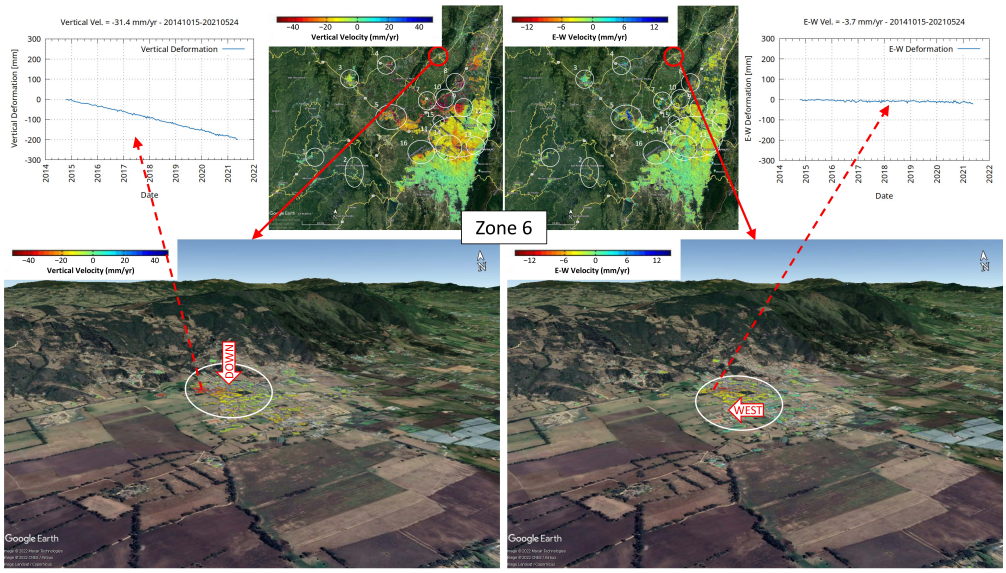


Figure 15. Time series results of the vertical and east–west deformation velocity rates for the municipality of Tenjo. Terrain subsidence is indicated by a white ellipse in this area.

Zone 7, as shown in Figure 16, corresponds to La Isla, which is located near Madrid, along with other municipalities that also experience subsidence effects such as Funza, Madrid, Mosquera, and Tenjo. The zone is surrounded by industrial buildings, greenhouses, and crop fields. According to the MT-InSAR analysis, vertical deformations of up to −20 mm/yr or even higher occur in this region, with values exceeding −40 mm/yr in

the surrounding areas. Furthermore, horizontal movements of 9 mm/yr to the east and −5 mm/yr to the west are observable.

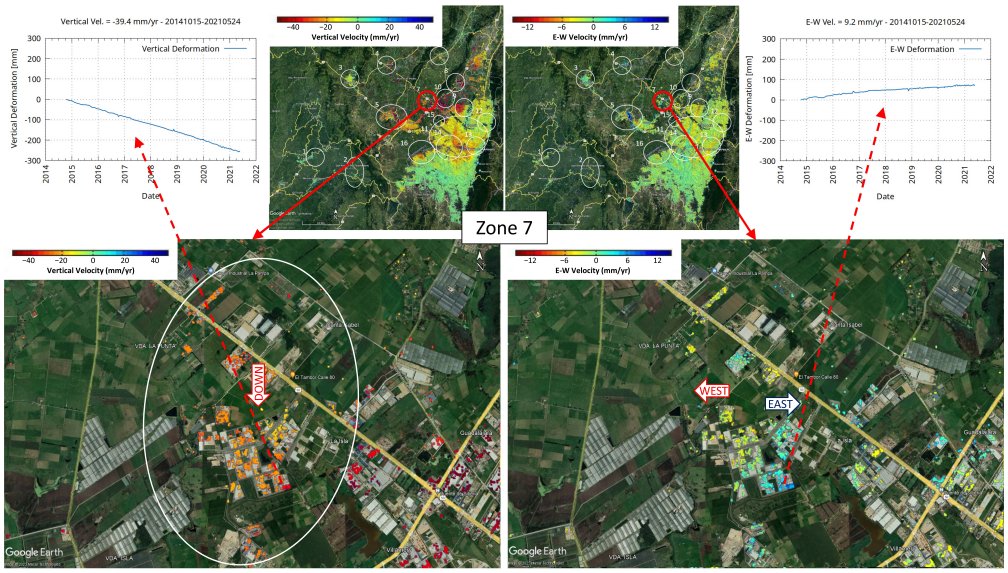


Figure 16. Time series results of the vertical and east–west deformation velocity rates for the Town of La Isla. In the area indicated with a white ellipse, ground subsidence with associated horizontal movements can be seen.

Figure 17 illustrates zone 8, which includes the municipalities of Cota and Chia. Cota is primarily dedicated to agriculture and is located in the foothills of the mountain range within the savanna region. The MT-InSAR analysis reveals vertical displacements ranging from −20 to −40 mm/yr in Cota and a similar subsidence pattern of −20 mm/yr in Chia. Figure 17 depicts two distinct trends of horizontal displacement observed in Cota: eastward and westward. On the contrary, Chia displays solely a horizontal displacement that heads toward the west.

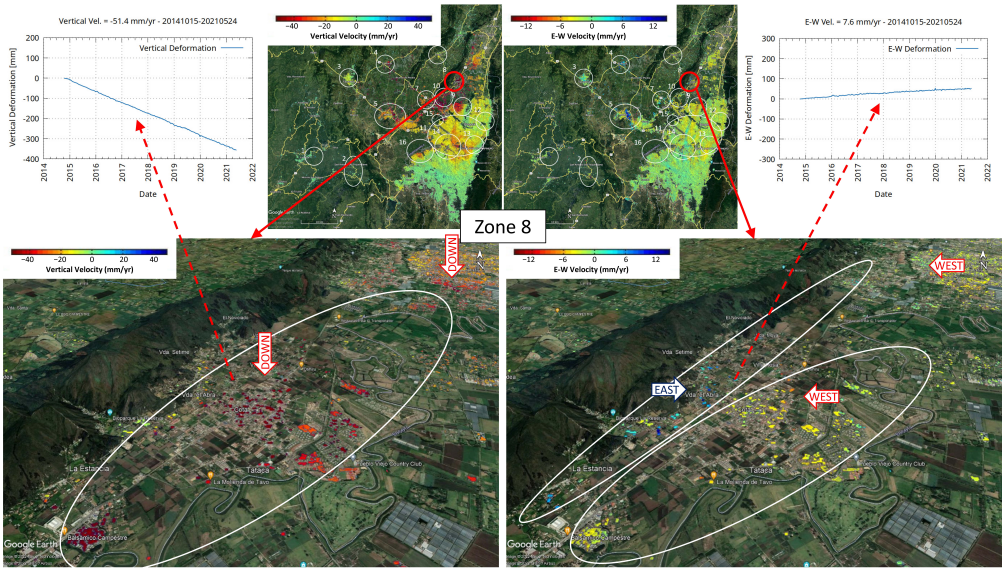


Figure 17. Time series results of the vertical and east–west deformation velocity rates for the municipality of Cota and Chia. The area marked with a white ellipse in the image on the left indicates a subsidence of the ground with its associated horizontal movements shown in the image on the right.

Zone 9, which is showcased in Figure 18, incorporates a group of neighborhoods found in the northwestern area of Bogotá, on the plain situated to the left of Suba Hill, deemed a secure area in light of the findings. This district is a combination of residential, commercial, and industrial properties. Vertical displacements range from −10 to −40 mm/yr. These may be due to various land uses such as groundwater extraction for industrial purposes, new residential development, or the influence of significant variations in regional piezometric levels on the foundations of older structures within the city. Figure 18 depicts two significant trends of horizontal displacement within this zone. One trend shows a distinct eastward movement with rates reaching up to 10 mm/yr. The other trend, smaller in scale, displays displacement in the opposite direction (west) with rates ranging up to −5 mm/yr. Furthermore, an area located on the outskirts of the city illustrates an eastward trend with rates of up to 3 mm/yr.

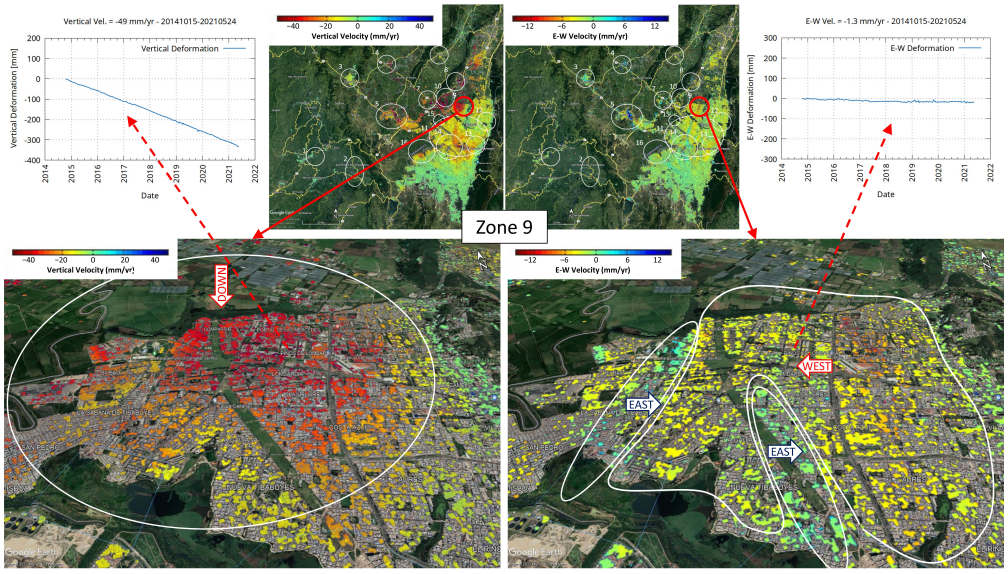


Figure 18. Time series results of the vertical and east–west deformation velocity rates of neighborhoods in the northwest of Bogotá city. In the image on the left, the white ellipse indicates a zone of significant subsidence, whose associated horizontal movements are indicated in the area on the right.

Figure 19 illustrates zone 10, which exhibits a vertical displacement trend equal to or greater than that of zone 7 in Figure 16. According to the SAR data, there are vertical displacements ranging from −20 to −40 mm/yr, with greater deformations. Horizontal displacements in this area reveal two patterns of movement toward the east and west, as Figure 19 shows.

The following Figures 20–25 depict the vertical and horizontal displacement trends within several neighborhoods of Bogotá (zones 11 to 16).

In zone 11, located within the city of Bogotá, Figure 20 illustrates the presence of an elongated corridor stretching from the center-west to the northwest. This area displays vertical movements akin to a passageway, fluctuating between −10 and −20 mm/yr. Moreover, horizontal displacement shows a tendency towards the east, with values reaching up to 5 mm/yr.

Moving on to zone 12, illustrated in Figure 21, it covers the Pedregal neighborhood situated alongside the Bogotá hills. The region comprises of a blend of residential and industrial areas. Vertical displacements observed in this zone range from 0 to −40 mm/yr. A noticeable eastward trend is present, resembling that of zone 11, which contrasts with the general trend observed in the city.

Figures 22–25 display similar subsidence patterns in vertical displacement, with rates ranging from −10 to −40 mm/yr in zones 13 to 16, respectively. In the Discussion section, Table 4 and Figure 32 offer a classification and demarcation of neighborhoods experiencing

deformations exceeding −20 mm/yr. The Santa Cecilia neighborhood in zone 14, situated at the center of the subsidence region, exhibits a vertical deformation rate of −25 mm/yr, in addition to westward displacements of up to −3 mm/yr. This area connects to zone 11, which is a lengthy passage that moves in the opposite direction.

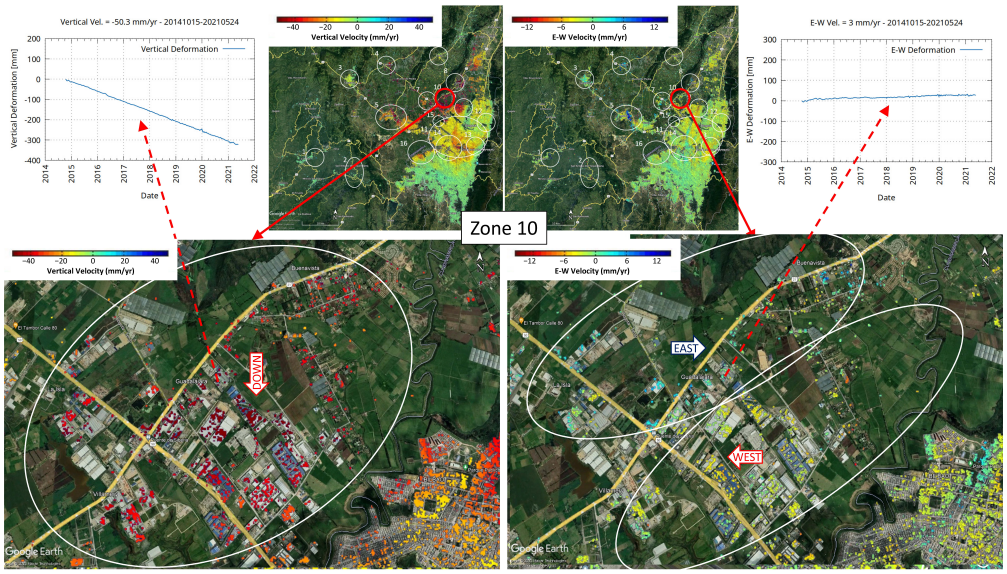


Figure 19. Time series results of the vertical and east–west deformation velocity rates of Guadalajara and Buenavista Town. In this area, a subsidence of the terrain can be seen, indicated by the white ellipse in the image on the left. This vertical movement is associated with horizontal movement, as shown in the image on the right.

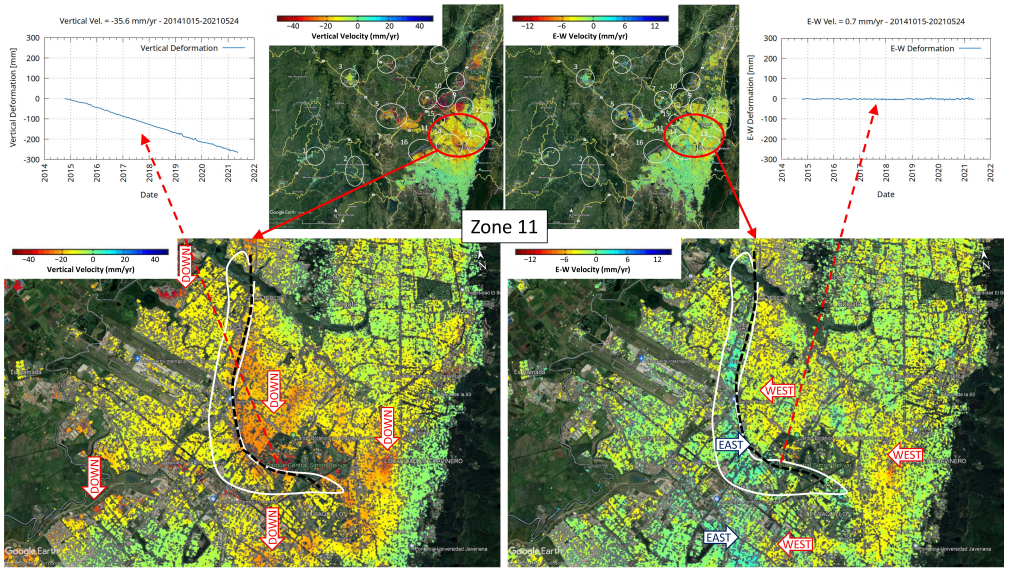


Figure 20. Time series results of the vertical and east–west deformation velocity rates in the middle of Bogotá city. In this zone, vertical movements with maximum values can be seen in the areas represented in orange in the left image. In the central zone, there is a longitudinal strip with a slightly pronounced horizontal movement, represented by the white polygon.

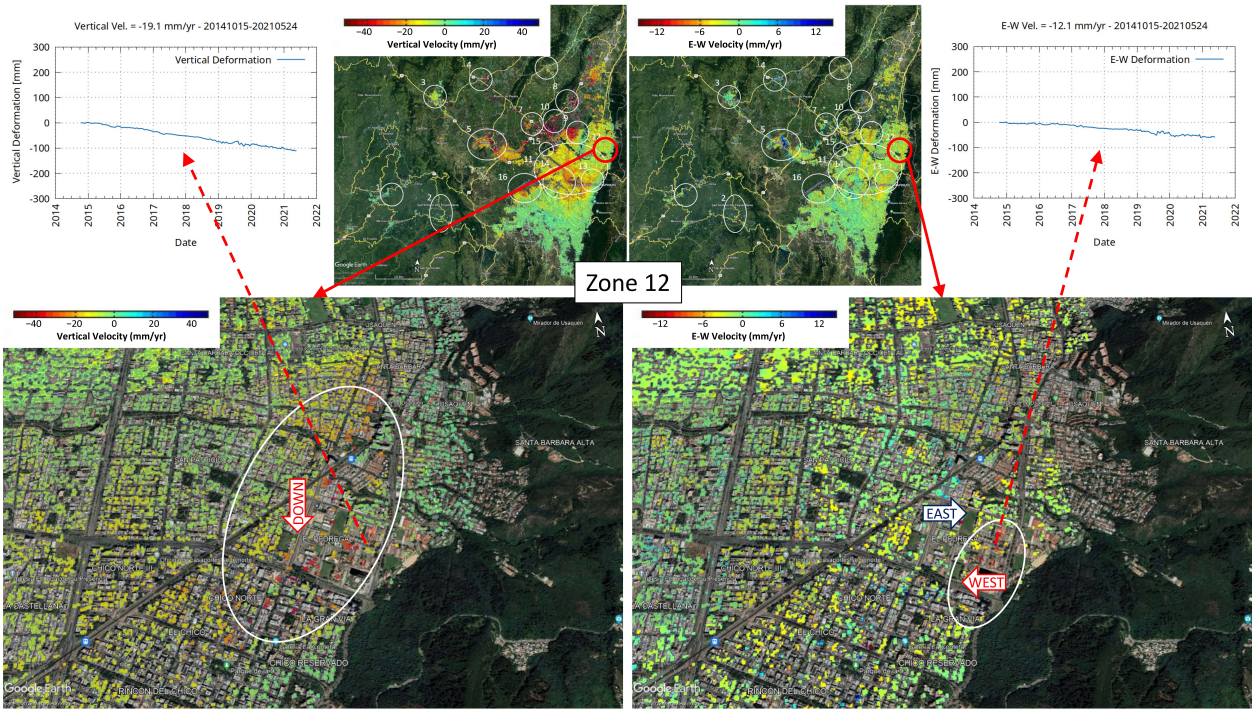


Figure 21. Time series results of the vertical and east–west deformation velocity rates of Pedregal neighborhood, located in the eastern part of Bogotá. The white ellipse defines an area with vertical ground motion and associated horizontal displacement.

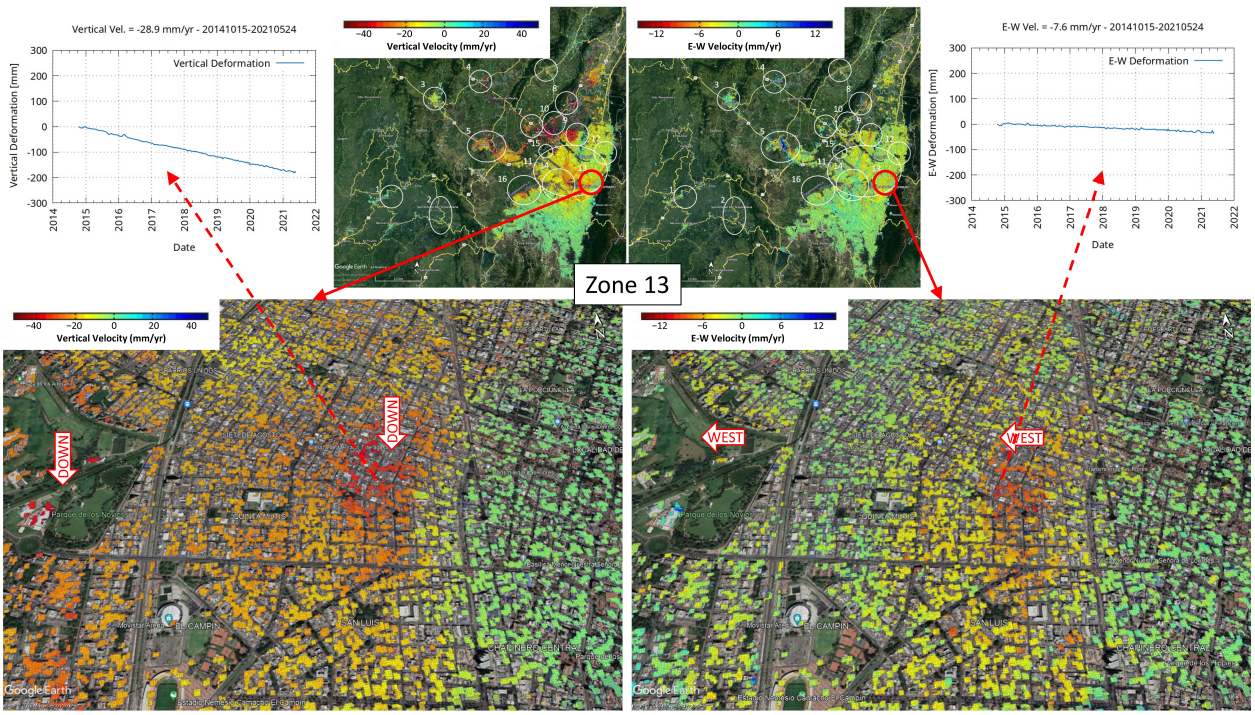


Figure 22. Time series results of the vertical and east–west deformation velocity rates for the Siete de Agosto neighborhood of Bogotá city.

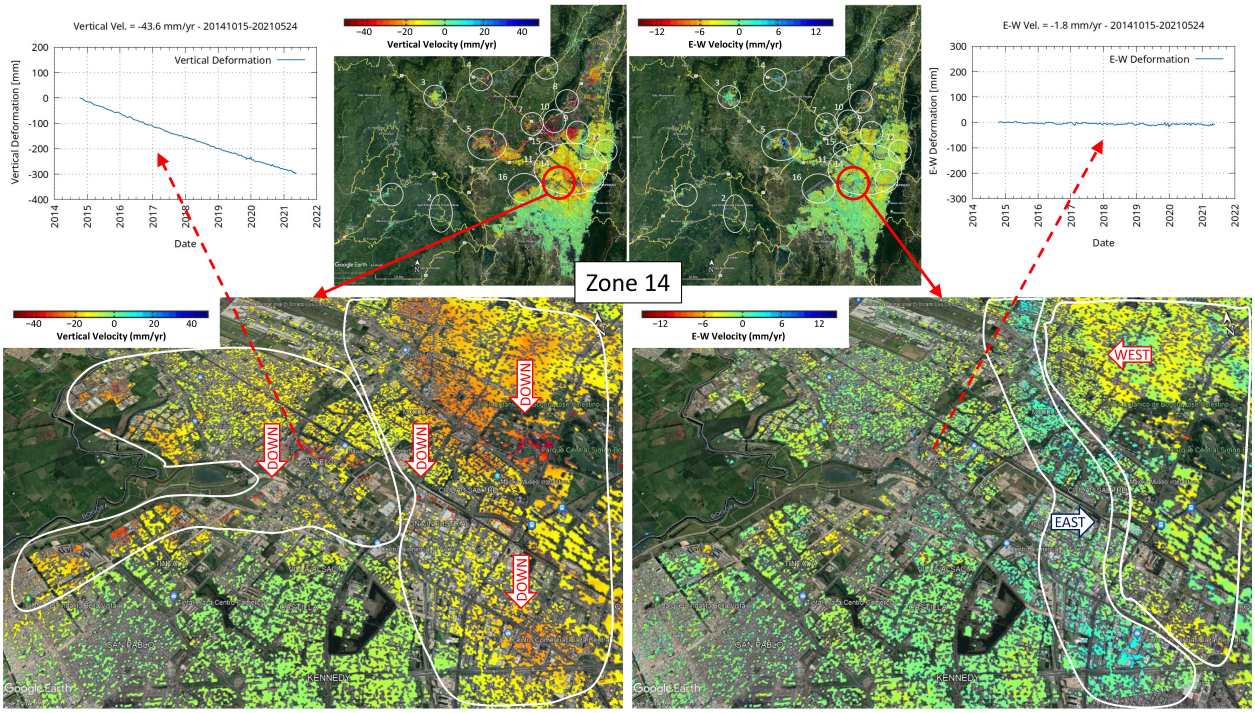


Figure 23. Time series results of the vertical and east–west deformation velocity rates located in a neighborhood from the center to the west of Bogotá city. Certain ground subsidence with differentiated horizontal movements can be seen in this area.

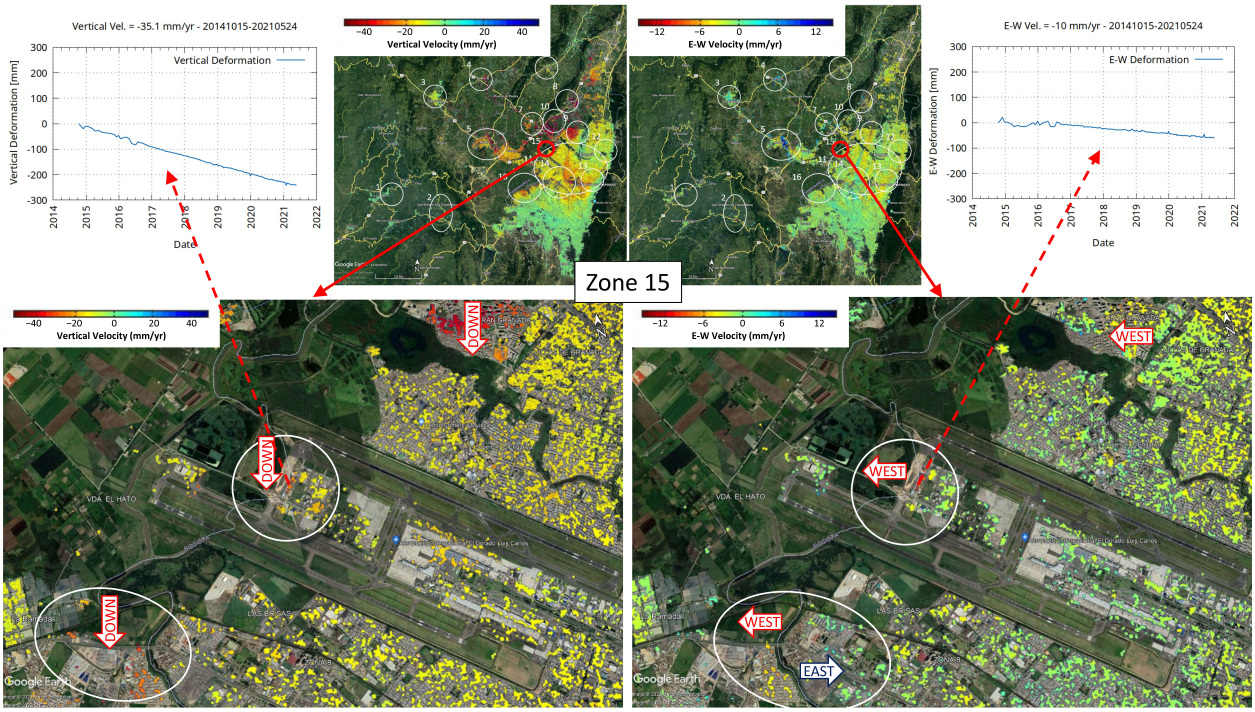


Figure 24. Time series results of the vertical and east–west deformation velocity rates for El Dorado Airport and the Florencia neighborhood.

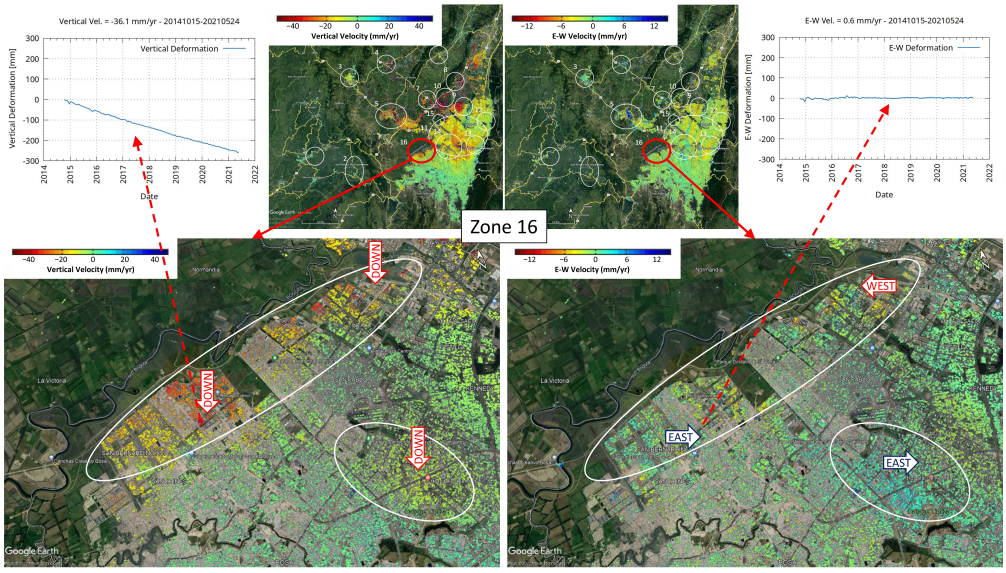


Figure 25. Time series results of the vertical and east–west deformation velocity rates for the Tintal del norte y sur neighborhoods group in the northwest of Bogotá city. The white ellipses indicate areas of pronounced subsidence and associated slight horizontal movement.

Table 4. Deformation rates of the neighborhoods significantly affected by the subsidence phenomenon in the central area of the Bogotá city (Figure 32).

Zone	Neighborhoods	Deformation Rates [mm/yr]		Description of Buildings Surroundings the Analysis Neighborhoods
		Max	Min	
1	Aeropuerto El Dorado	−11.6	−4	
2	Álamos	−24.4	−2.5	Warehouses Area and Residential Buildings
3	Bavaria	−15	−2	New Residential Buildings
4	Bolivia	−19	−4.3	New buildings; Residential Buildings Area
5	Boyacá Real	−23	−5	Residential Buildings Area
6	Calandaima	−29	0	New Residential Buildings
7	Capellanía	−17.6	−4.7	Warehouses Area and Residential Buildings
8	Castilla	−12	−1	
9	Chicó Lago	−20	0	Residential Buildings
10	Ciudad Salitre Occidente.	−24	−1	Residential Buildings
11	Ciudad Salitre Oriente.	−27.7	−5.8	Residential Buildings and Warehouses Area
12	Doce de Octubre	−24	−5	Residential Buildings
13	El Porvenir	−26.6	0	New Residential Buildings
14	Engativá	−17.1	−5	Warehouses Area and Residential Buildings
15	Fontibón	−35.4	−4.4	Warehouses Area and Residential Buildings
16	Fontibón San Pablo	−16.5	−2.6	Warehouses and Industrial Area
17	Galerias	−22.6	−1.9	Residential Buildings
18	Garces Navas	−37.1	−5	New Residential Buildings
19	Granjas de Techo	−33.1	−2	Warehouses Area
20	Jardin Botanico	−30	−8.2	Residential Buildings and Sports Areas
21	La Esmeralda	−23	−5	Residential Buildings
22	Las Ferias	−26.1	−1	New Residential Buildings
23	Los Alcazares	−31	−3.7	Warehouses Area and Residential Buildings
24	Minuto de Dios	−14	0	Residential Buildings
25	Modelia	−17	−3.7	Residential Buildings
26	Parque salitre	−38.1	−9.6	Parks; Green area; Residential area
27	Parque Simon Bolivar	−28.1	−10	Parks; Green area; Residential area
28	Patio Bonito	−20	0	
29	Puente Aranda	−23	−6	Factories and Warehouses
30	Quinta Paredes	−21.3	−1	Residential Buildings
31	Santa Cecilia	−25.3	−9	Residential Buildings
32	Teusaquillo	−18.8	0	Residential Buildings
33	Tintal Norte	−27	0	
34	Tintal Sur	−18.9	−2	Warehouses Area and New Residential Buildings
35	Zona Franca	−24.5	−1.2	Warehouses Area and New Residential Buildings

4.2. GNSS and Comparison with MT-InSAR

Figure 26 displays the time series of GNSS stations (ABCC, BOGA, and BOGT) since their commissioning; that is, they have recorded data for a period of approximately 22 years. BOGA and BOGT stations show a linear trend of cumulative deformation in the height component over the entire period, with values of around −861 mm and −641 mm, respectively. In contrast, ABCC started recording data in SIRGAS in August 2011 and has displayed a consistent downward deformation trend of around −197 mm in its height component up to 2021 (Figure 26c and Table 5). The deformations in the east component of these stations have shown relative stability over time, as observed in Figure 26b. For a more comprehensive understanding of the GNSS stations, readers can refer to previous research studies [51,54–56].

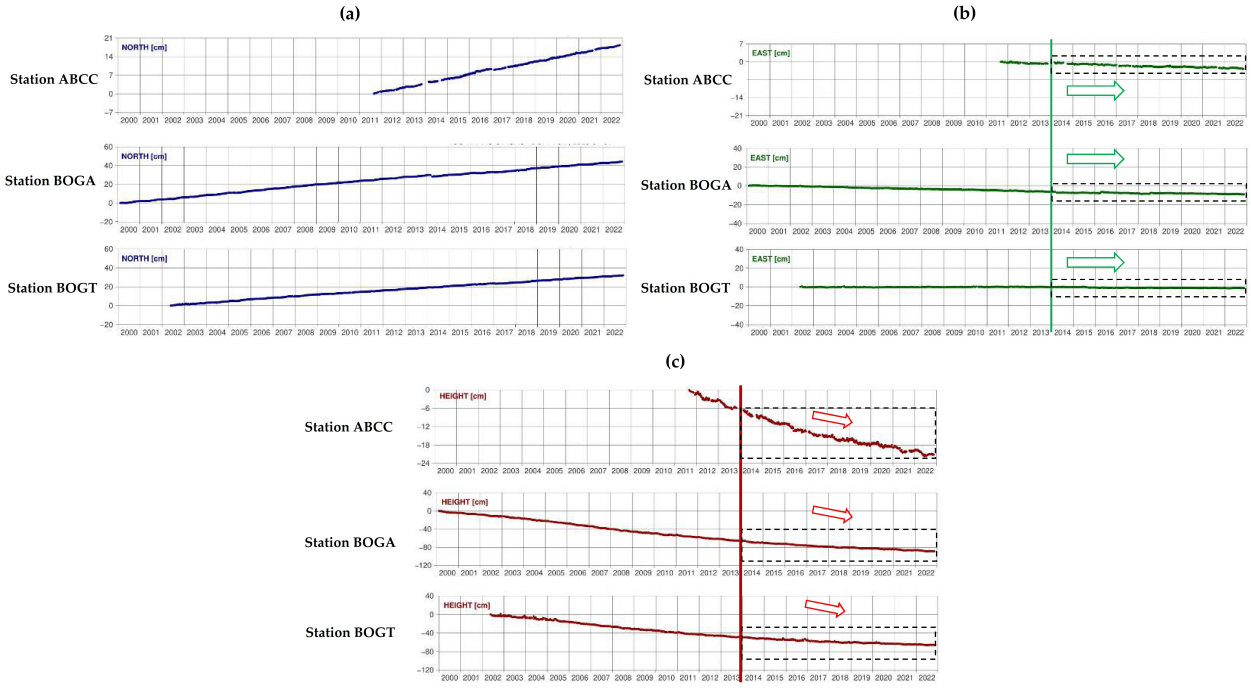


Figure 26. Position time series of ABCC, BOGA, and BOGT GNSS stations in Bogotá from 2000 to 2021, processed by SIRGAS–CON. (**a**) North component. (**b**) East component. (**c**) Height component. Note: The dashed lines on graphs (**b**,**c**) indicate the duration of our study throughout the complete time series of the GNSS stations. The arrows indicate the direction of the time series trend. (Source: https://sirgas.ipgh.org/red--gnss/estaciones/lista--de--estaciones/, accessed on 1 October 2023).

Table 5. Cumulative displacement of positions for GNSS stations based on their geodetic observations as reported on the official website between January 2000 and December 2021. (Source: https://sirgas.ipgh.org/red--gnss/estaciones/lista--de--estaciones/, accessed on 1 October 2023).

GNSS Station	North [mm]	East [mm]	Up [mm]
ABCC	170.69 ± 0.061	−23.36 ± 0.115	−197.06 ± 0.213
BOGA	427.51 ± 0.029	−85.80 ± 0.045	−861.84 ± 0.081
BOGT	309.28 ± 0.051	−12.65 ± 0.116	−641.12 ± 0.192

Figure 27 shows a portion of the cumulative vertical displacement map from Figure 7 overlaid with the positions of three GNSS stations. An analysis of the station components confirms the existence of a trend of subsidence in specific areas of Bogotá, with deformation rates increasing over time. The use of MT-InSAR has enabled the creation of a detailed map of the city, which shows an increasing trend in deformation rates in certain neighborhoods during the study period. This trend was not identified in previous studies.

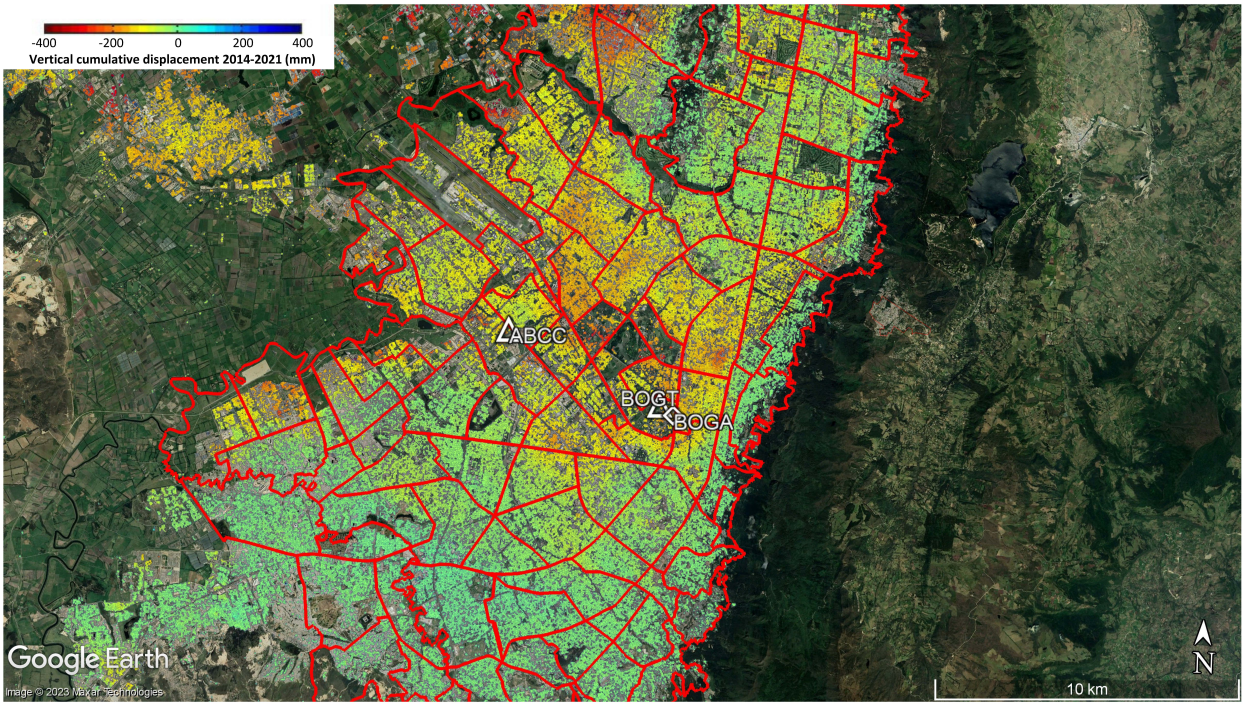


Figure 27. ABCC, BOGA, and BOGT GNSS stations are depicted on the MT-InSAR vertical cumulative displacements map as white triangles.

To align with the MT-InSAR processing results, we adjusted the time period for the time series of the three GNSS stations between 2014 and 2021. Figure 28 displays the component adjustments of the GNSS stations during this period, with 2014 as the baseline year. We obtained the weekly positions of ABCC, BOGA, and BOGT from 2014 to 2021 from the SIRGAS website.

The GNSS station ABCC is located in the neighborhood of Granjas del Techo, and as shown in Figure 28, its height component indicates a cumulative displacement of −140 mm (−17.5 mm/yr) during our study period. Figure 27 MT-InSAR results demonstrate that the displacement ranged from −100 to −150 mm (−12.5 to −18.8 mm/yr) and exceeded those values in some adjacent regions. The eastern station component, as depicted in Figure 28, indicates values of approximately −22 mm (−2.8 mm/yr), while the east–west MT-InSAR results suggest a cumulative displacement value ranging from −10 to −20 mm (−1.3 to −2.5 mm/yr) (Figure 7b).

The BOGA and BOGT stations are located in the Simón Bolívar Park neighborhood. Their height components (Figure 28) show accumulated displacements of −210 mm (−26.2 mm/yr) and −160 mm (−20 mm/yr), respectively. The MT-InSAR results depicted in Figure 27 reveal that there were accumulated deformations that ranged from −170 to −200 mm (−21.2 to −25 mm/yr) in the vicinity and neighborhood of the stations. Specifically, in the eastern component of the stations, BOGA exhibited a deformation of −27 mm (−3.4 mm/yr), while BOGT showed a deformation of −13 mm (−1.6 mm/yr) from 2014 to 2021, as presented in Figure 7b. In this neighborhood of the city, Figure 7b shows identifiable MT-InSAR deformation values ranging from 0 to −30 mm (−3.7 mm/yr).

Ultimately, both techniques have indirectly confirmed consistent results in detecting observed deformations in these locations. The SIRGAS results and MT-InSAR outcomes have both been effective.

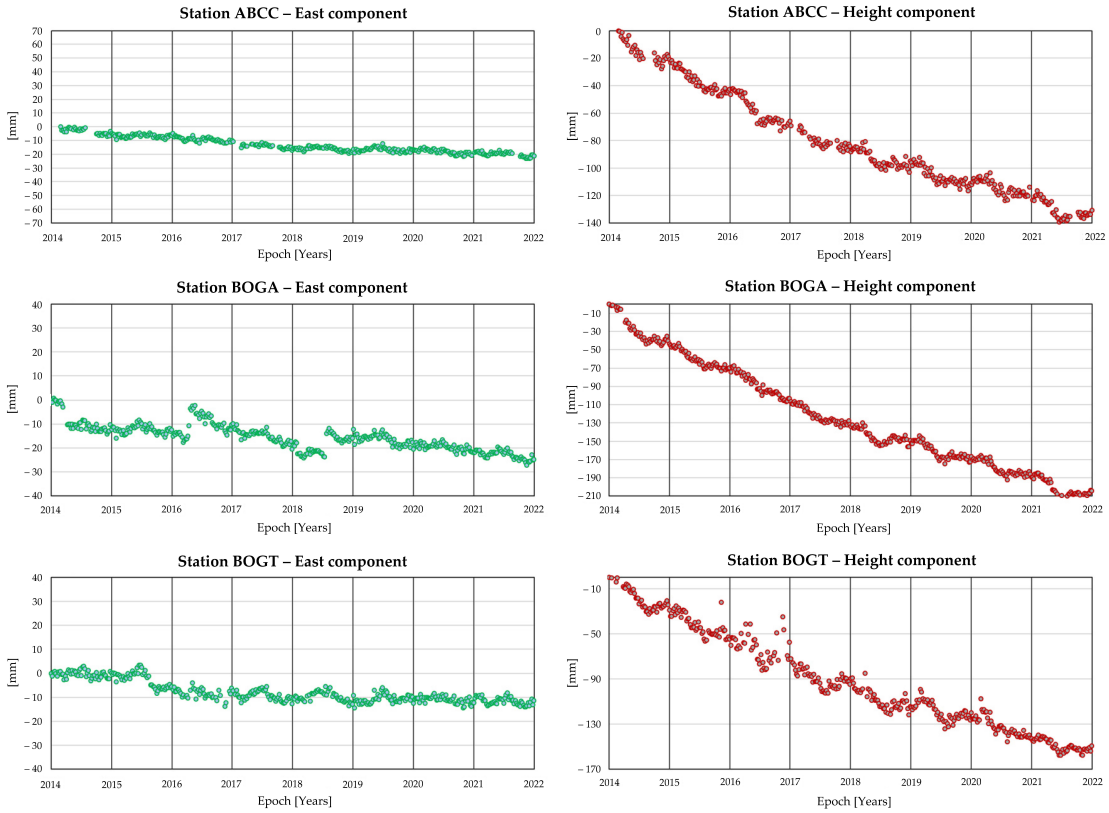


Figure 28. Positions of the ABCC, BOGA, and BOGT GNSS stations in the east and height components indicated by the dashed lines in Figure 26b,c for the period 2014 to 2021.

5. Discussion

This section presents a thorough analysis of the MT-InSAR analysis results in areas where subsidence triggers have occurred in the Bogotá savanna and city. The analysis is compared with the GNSS data. This investigation is closely linked to CAR's groundwater management plan. Hydrogeological sub-basins in the region have recorded a gradual decline in water levels in both the Quaternary and Guadalupe aquifers. Over-pumping of water from aquifers is the main cause of subsidence triggers, resulting in a reduction in piezometric levels between 5 and 40 m in various sub-basins of the Bogotá savanna. Despite a lack of hydrogeological or updated GNSS data for the region, the use of Sentinel-1 imagery and MT-InSAR techniques has allowed for an updated measurement of deformation rates in 2021, providing a contemporary understanding of this phenomenon. The municipalities most impacted by this phenomenon are Madrid, Mosquera, Funza, areas surrounding Facatativá and Cota, and Chia. These areas demonstrate a linear trend of vertical cumulative displacement values of −200 mm from 2014 to 2021, with an average subsidence rate ranging from −30 to −40 mm/yr reaching values close to −60 mm/yr. The region of Facatativá has received significant attention from researchers and governmental organizations regarding the extraction of groundwater from the Guadalupe and Quaternary aquifers, prompted by various economic activities performed by local industries.

Our study introduces a new pattern of Bogotá savanna deformation obtained through the use of MT-InSAR. This is the first time that these deformations have been visualized in such a way. Prior research conducted by several institutions and authors depended on traditional monitoring methods, highlighting the significance of our results for the comprehension of this phenomenon. Additionally, Figures 10–25 illustrate 16 zones with significant deformation, of which 10 exhibit noteworthy deformations throughout the study area, including La Mesa, San Antonio de Tequendama, Facatativá, El Rosal, Madrid, Tenjo, la Isla, Cota and Chia, Guadalajara, and Buenavista. Some of these areas have undergone subsequent studies examining the reduction in potentiometric levels, such as Facatativá or

El Rosal, conducted by various authors. The observed trend of subsidence in these areas in recent years has been attributed to the extraction of groundwater for agricultural or industrial purposes. However, the image analysis also identified other factors, such as accelerated construction of housing, that could potentially contribute to this trend. The rapid construction of housing structures, factories, and businesses in the Bogotá savanna region has caused excessive loads on the highly compressible soft clays, resulting in early consolidation effects on the savanna soils. The impacts of primary consolidation from these structures can last for multiple years, as seen in the Sentinel–1 analysis during our study period. This phenomenon is caused by the gradual spread of loads on the foundation, leading to subsequent impacts on the underlying soil. Lowering of the water table and vegetation suction contribute to subsidence, leading to clay shrinkage in Bogotá and damaging civil structures nearby. The observed subsidence trend was mainly concentrated in the central and southwestern regions of the savanna in alignment with documented localized subsidence patterns in the Quaternary and Guadalupe aquifer systems. This information is reported by [21,24,26,27,30,57] and presented in Table 2 and Figures 2 and 29.

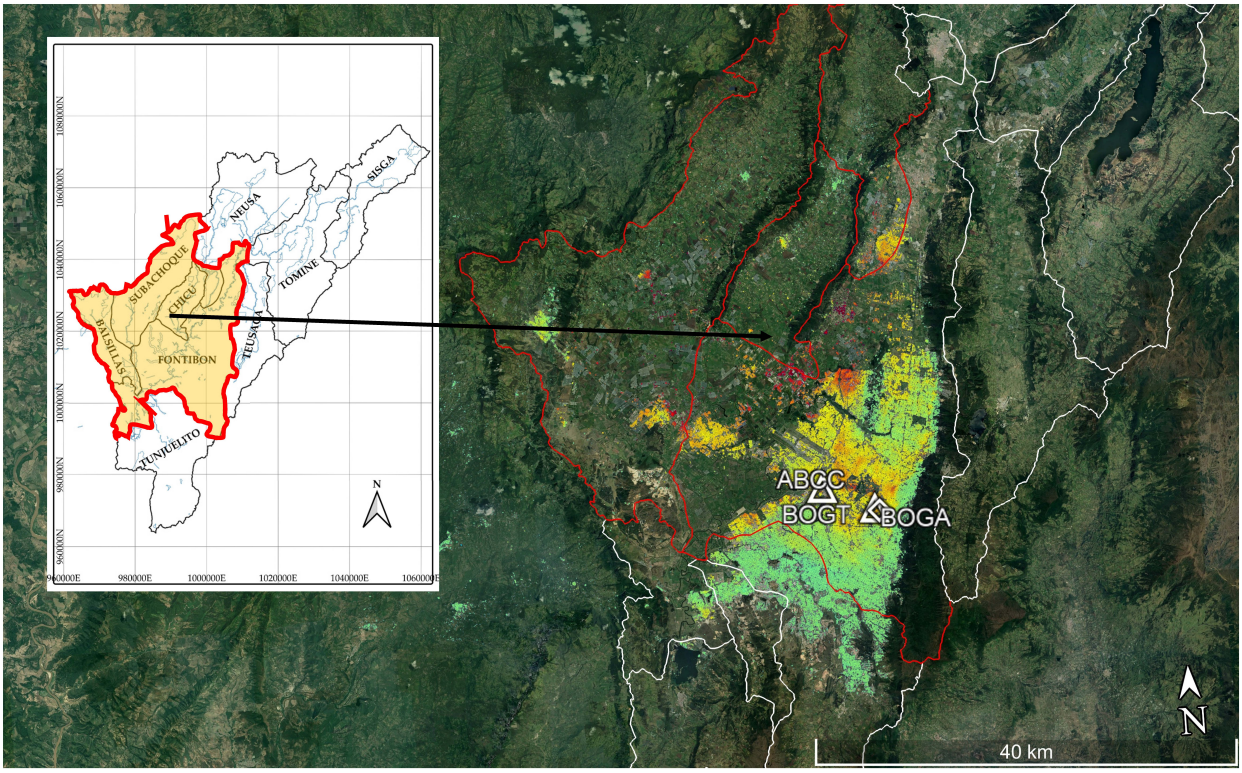


Figure 29. Region of land subsidence in the savanna, superimposed on the sub-basins with low piezometric levels (as shown in Table 1), which is associated with this phenomenon, according to a study conducted by CAR [30].

In 2005, an agreement by CAR (the environmental authority in Colombia) identified certain municipalities, including Tenjo, El Rosal, Madrid, Funza, Facatativá, and Mosquera, as well as parts of Cota, Tabio, Subachoque, Soacha, and Sibaté, as critical areas for groundwater exploitation. These areas were delineated within the boundaries specified in two polygons (1 and 2) [30].

As illustrated in Figure 30, which shows these polygons outlined by CAR alongside the MT-InSAR results, significant ground deformation persists in the Bogotá savanna, particularly within the critical areas identified by CAR. During our study period, vertical deformations of up to −400 mm were observed. This indicates that land subsidence in the Bogotá savanna, under monitoring since the 1990s, remains a persistent challenge in the region and is extending beyond the initially identified polygons.

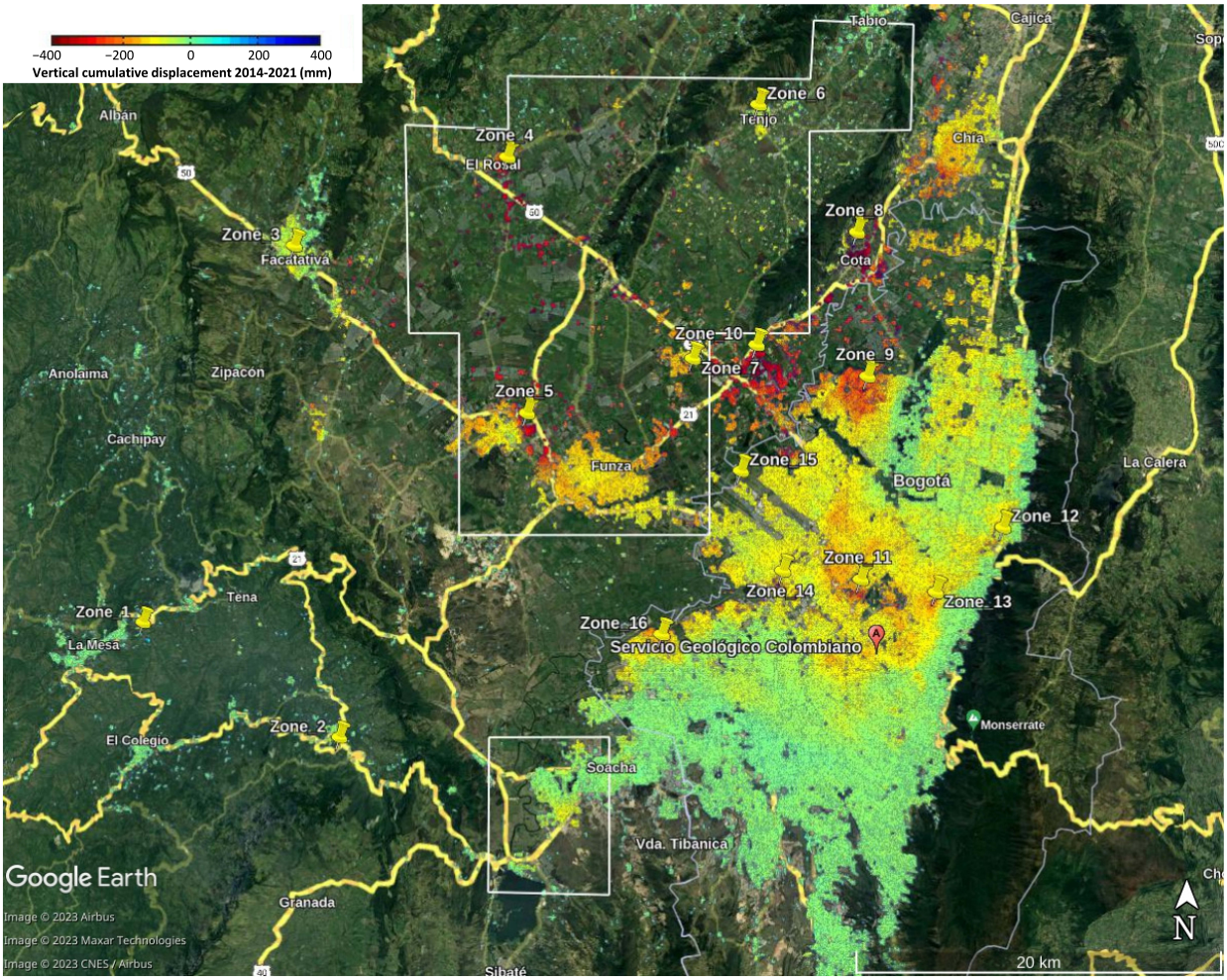


Figure 30. Polygons 1 and 2 (in white color) delimiting areas identified as critical areas for exploiting groundwater by CAR in 2005 [30].

Overall, the deformation rates across the savanna area indicate a greater vertical deformation trend compared to the horizontal, which is evident in Figures 7 and 8.

The horizontal deformations identified are a result of secondary displacement caused by land subsidence. Subsidence events only occur in areas with surface topographic variations and do not seem to be linked to deeper geological characteristics. This is because the underlying syncline basin should produce consistent and convergent movements, yet what is observed are motions in different directions that are consistently associated with the slope of the land where subsidence takes place. The horizontal displacements are typically 15% to 25% of the magnitude of the vertical displacements, increasing with higher rates of subsidence and steeper slopes.

As previously mentioned, research on Bogotá's subsidence dates back to the 1990s, when the city underwent seismic microzoning analyses. Various geotechnical, hydrogeological techniques, and GNSS networks were utilized in subsequent investigations to study subsidence in the entire metropolitan area, confirming its presence in different locations within the city. In 2009, FOPAE and ICC collaborated on a study analyzing the effectiveness of DInSAR as an assessment tool for monitoring deformation phenomena [20]. For this study, a dataset consisting of eight ENVISAT images from 2008–2009, two images from 2002–2003, and an additional eight images from 1997 to 2006 obtained from a later study was used to generate 57 interferograms. The ICC algorithm was used to carry out multi-temporal analysis during the study period of October 1997 to March 2009. The results successfully identified the main subsidence focus of the Puente Aranda area, which had a

deformation rate of −75 mm/yr (Figure 31a) [20]. Another study, as documented by Mora Páez et al. [22], used TerraSAR-X radar images for the quantitative analysis of subsidence in Bogotá. The resulting deformation map showed that the central region of the city had a deformation rate of up to −33 mm/yr (Figure 31b).

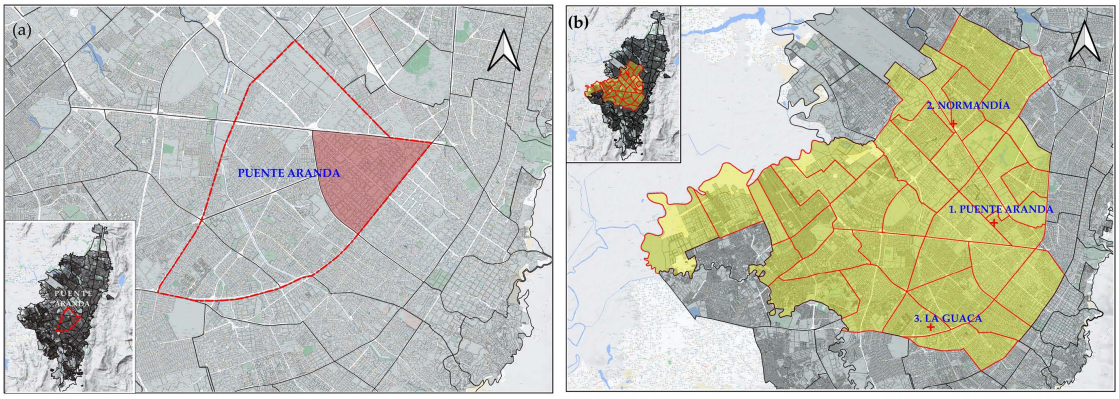


Figure 31. (**a**) Urban area in the city of Bogotá centered on the Puente Aranda neighborhood showed high linear velocity rates between 1997 and 2009, as observed using ENVISAT images (Source: [20]). (**b**) Another study focused on three sites in Bogotá with varying degrees of subsidence between 2011 and 2017, including the highest (Puente Aranda), medium (Normandia), and low (La Guaca), as calculated from TerraSAR-X images (Source: [22]).

We compared our results obtained from Sentinel-1 images with previous studies [20,22] to assess the spatiotemporal evolution of subsidence in Bogotá. This verification process enabled us to gain insights into the subsidence changes and patterns over time.

We analyzed neighborhoods in the central region of Bogotá (Figure 32) and found subsidence appearing to extend from the city center towards the north, south, and west by utilizing MT-InSAR processing. Our study identified 35 areas (Table 4) with notable yearly deformity rates in this city region.

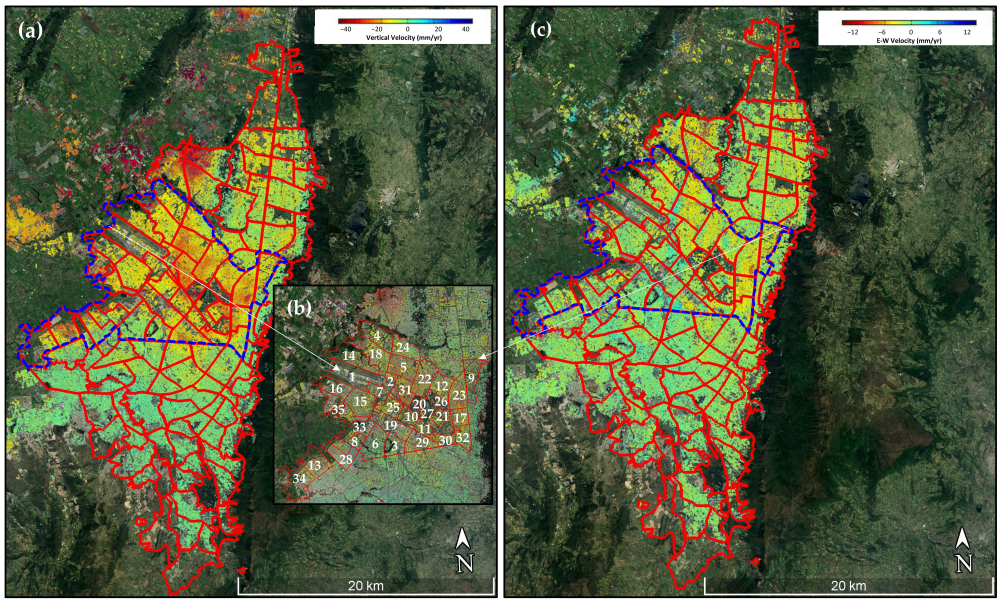


Figure 32. (**a**) The blue dashed lines enclose a sizeable area of subsidence, indicating vertical displacement in Bogotá's city center. (**b**) The highlighted area indicates neighborhoods (Table 4) classified within the zone of vertical displacement. (**c**) The dashed lines enclose a considerable area of displacement, indicating an east–west direction in Bogotá's city center.

We separated various neighborhoods with subsidence exceeding −20 mm/yr. Some of these neighborhoods, including No. 2, 20, 25, and 31, situated in the city's central area, indicated lowered vertical deformation rates, reaching from −17 to −30 mm/yr, when compared to the previous study. Nonetheless, we noted a rise in deformation rates in regions near the subsidence center. The vertical deformation rate in Fontibón neighborhood (15) was −35.4 mm/yr, Garcés Navas neighborhood (18) showed −37.1 mm/yr, Granjas de Techo neighborhood (19) exhibited −33.1 mm/yr, and Salitre Park (26) displayed −38 mm/yr. This indicates that while the deformation trend decreased in certain areas of the central region, subsidence is expanding towards the peripheral neighborhoods of the central subsidence focus.

To validate the vertical accumulated displacement using geodetic techniques, we utilized two reference areas from previous studies: Granjas de Techo and Simon Bolivar Park. These areas contain three GNSS stations, specifically BOGT, BOGA, and ABCC. The vertical and east velocities of these stations derived from GNSS demonstrated agreement with MT-InSAR results, as indicated in Section 4.2.

Additional research conducted by Kaniuth et al. [54] using BOGT and BOGA stations located in Bogotá D.C. obtained a vertical component value of -25.2 ± 1.4 mm/yr for BOGA, assuming an identical rate for BOGT. This was based on the analysis and processing of GPS data from 2000–2001. Rudenko et al. [55] conducted a thorough reprocessing of GNSS data from the period 1998 until 2007, revealing a vertical component rate of -44.21 ± 0.19 mm/yr, nearly double the rate determined by Kaniuth et al. Additionally, the latest GPS data studies from the BOGT GNSS station, conducted by the SGC, have produced a time series of the vertical component that shows a continuous downward trend, corresponding to a linear trend estimate of the rate of -34.5 ± 0.9 mm/yr [19].

As mentioned before, numerous studies have investigated the subsidence phenomenon in Bogotá since the 1990s. For example, the study "Advances in subsidence studies in Bogotá city" by Ávila and Castro-Villamarín [21] was conducted in 2011 and used piezometric level variations recorded over 15 years to model subsidence magnitudes and project future trends. The study evaluated subsidence caused by water table declines at a rate of 0.1 m/yr using a "soft-soil" model at two locations: El Dorado Airport and the INGEOMINAS site (Figure 33). This model employed an elastoplastic analysis of the consolidation process. This rate of 0.1 m/yr was selected due to limited variability intervals deduced from available soil studies, given the strong association between groundwater levels and local climatic factors. Subsidence evolution at these sites over 100 years was analyzed under four scenarios of water table declines at a rate of 0.1 m/yr: a decline lasting 5 years (green curve), 10 years (blue curve), 20 years (pink curve), and 50 years (red curve). According to the model, cumulative land subsidence of up to −175 cm (−17.5 mm/yr) was anticipated at INGEOMINAS and −300 cm (−30 mm/yr) at El Dorado Airport in the most extreme scenario (red curve). In the least extreme scenario (green curve), cumulative land subsidence over 100 years at both sites was predicted to be around −20 cm (−2 mm/yr).

The model estimated subsidence at INGEOMINAS to be between −80 and −125 mm (−12––15.6 mm/yr) and at El Dorado Airport around −50 mm (−7.5 mm/yr) during the first 6.6 years (the period of our MT-InSAR analysis). When comparing these predictions with the accumulated vertical deformation obtained through MT-InSAR over a 6.6-year period (Oct 2014–May 2021), our study found that the cumulative vertical deformation at INGEOMINAS was −66 mm (−10 mm/yr) and −80 mm (−12 mm/yr) at El Dorado Airport (blue arrows in Figure 33). Our results were used to calibrate the model, revealing a slight overestimation of settlement at INGEOMINAS and a slight underestimation at El Dorado Airport. However, in both cases, the subsidence rates were relatively similar during this 6.6-year period.

To illustrate the impact of instability on building structures and settlements in a commercial area, this study presents two case studies from different regions of Bogotá. The first example details a survey conducted in 2019 in a residential complex located in the western part of the Ciudad Salitre neighborhood of Bogotá city (Figure 34) by

Surveying Engineer Gustavo Matiz, Civil Engineer Leonardo Ruiz Arce, and Architect Jorge E. Ruiz Bastidas. The survey detected settlements ranging from −4 to −8 cm in various positions within the building structure. These findings corresponded with the results of the MT-InSAR analysis, which demonstrated a vertical deformation rate of approximately −24 mm/yr in the vicinity over the study period, as shown in Table 4. However, the majority of the deformations were attributed to the consolidation process resulting from the vertical loads of the building, suggesting that intensive construction can contribute to regional subsidence.

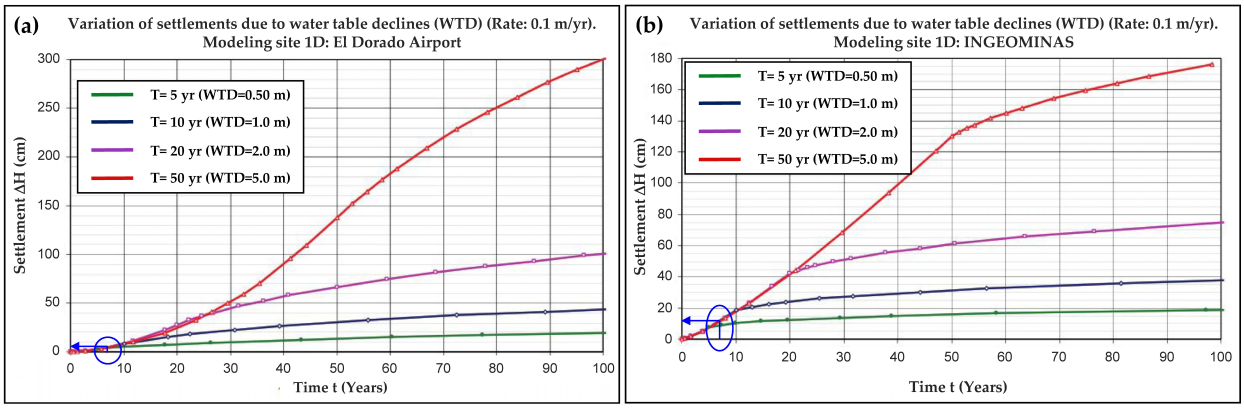


Figure 33. Subsidence model prediction according to a water table drawdown at a rate of 0.1 m/yr during different periods. The blue arrows indicate the settlement predicted by the model for a 6.6-year period, coinciding with the MT-InSAR analysis period. (**a**) El Dorado Airport sector. (**b**) INGEOMINAS sector. Source: [21].



Figure 34. Structural pathologies of a building in 2019 in a subsidence zone (western part of Ciudad Salitre) in the city of Bogotá. The images were provided by Gustavo Matiz (Surveying Engineer), Leonardo Ruiz Arce (Civil Engineer), and Jorge E. Ruiz Bastidas (Architect).

Structural reinforcement measures were subsequently implemented; however, occupants reported additional damage to the pipes and cracks in the walls. The identified damages were found to be residual stresses caused by the initial settlement of the structure. They do not present a risk of building collapse in the residential complex.

The second example (Figure 35) concerns settlements in the Chicó Lago neighborhood that impact numerous buildings. This area was once characterized by extensive lakes and forests, but with the urban development of Bogotá, the lake was drained, and the land was developed. MT-InSAR results reveal deformation rates ranging from 0 to −20 mm/yr in this area. However, local consolidation processes in the constructed areas are lower than the regional subsidence process. Conclusions drawn from such results must be interpreted with caution due to the declining tree cover in the area. Steps were constructed for building access, as shown in Figure 35. This can be attributed to the use of driven floating piles, which increase soil density and transfer load to deeper layers, reducing the consolidation rate.

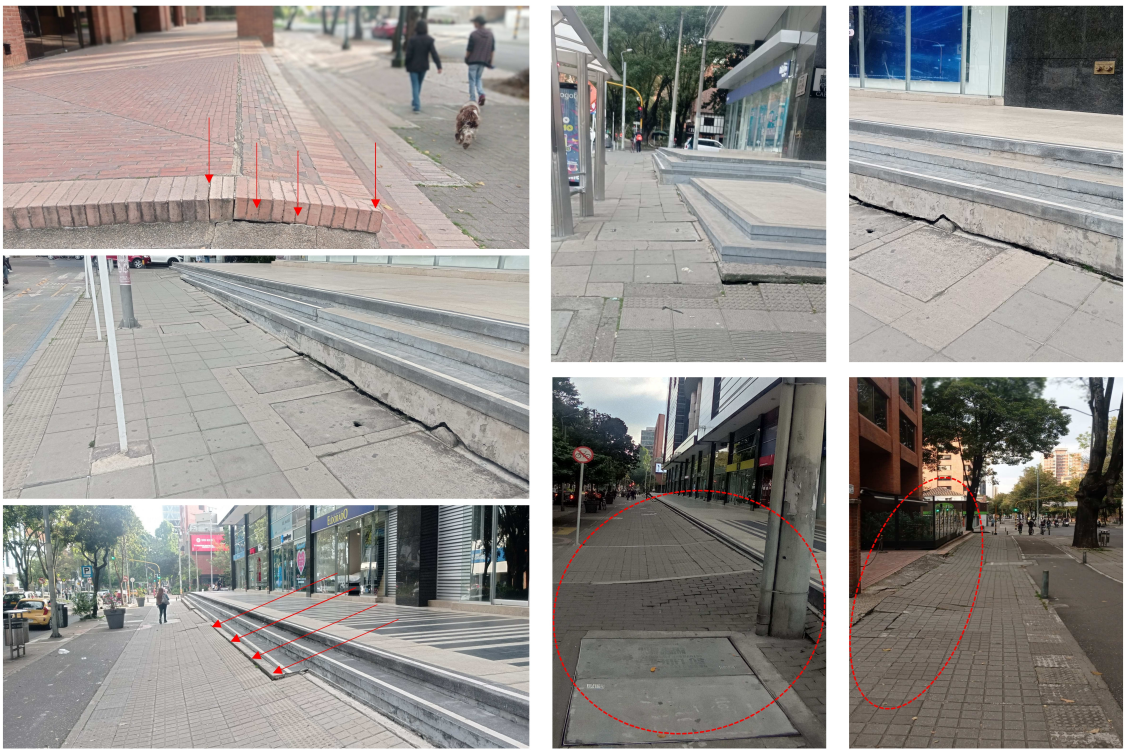


Figure 35. Effects of settlements on the pedestrian walkways around a mall in the Chicó Lago neighborhood.

Extensive inspections were conducted throughout the study area, including the capital city, and no discernible effects of subsidence were observed in the regions experiencing the highest subsidence rates. These effects could have included ground deformation, building deterioration, or structural cracking. This may be attributed to the minimal occurrence of differential settlements over a large area, making it challenging to discern the impact of subsidence on the affected structures.

6. Conclusions

This study conducts an MT-InSAR analysis of Sentinel-1 data from 2014 to 2021, in addition to utilizing GNSS data as a verification technique. Furthermore, past hydrogeological and geotechnical data were included. The main goal is to explore subsidence in the Bogotá savanna and city and identify novel factors contributing to this phenomenon. Consequently, we draw the following conclusions:

- The subsidence phenomenon in the AOI continues to be active today, mainly impacting the central and western regions of Bogotá savanna, as well as certain areas within Bogotá city. Groundwater over-exploitation, driven by industrial development and population growth, is regarded as the cause of this subsidence, which has been present since the 1990s. Several municipalities, including El Rosal, Madrid, Facatativá, Cota, Funza, Bojacá, and others, demonstrated substantial cumulative deformation up to −400 mm during the research period from 2014 to 2021.
- The subsidence indicates deformation velocity rates ranging from −10 to −40 mm/yr in the central and western areas of the Bogotá savanna, with some places even higher (−60 mm/yr). Horizontal deformation rates in the east–west direction (around 12 mm/yr) are lower than the vertical rates within the AOI. However, it is critical to highlight that this still poses a significant problem that necessitates constant surveillance in the region. The Quaternary and Guadalupe aquifers show continually decreasing deformation rates, suggesting a decline in the region's groundwater potentiometric level. Such depletion results from intensive extraction for basic consumption needs surpassing natural recharge. Consequently, surface layers compact and subside, leading to rapid damage and deterioration of pavements in Bogotá savanna and Bogotá city.
- The MT–InSAR processing results reveal that, like the savanna, Bogotá experiences deformation rates in different neighborhoods situated in the north, center, west, and some parts of the south. Previous studies have identified deformation rates of up to −33 mm/yr in specific neighborhoods of the city. Even greater deformation rates and a spatiotemporal expansion from the city center towards the south, north, and west were observed in our latest analysis.
- Conversely, the central area of Bogotá experienced a consistent downward movement over the period from 2014 to 2021, as confirmed by both MT-InSAR and GNSS data from the SIRGAS stations, providing additional validation across a significant portion of the city. Continuous monitoring of subsidence in the capital is recommended, due to the extensive area covered within the city, which could pose a risk to the stability of structures.
- Additionally, the study found that the increasing demand for housing in smaller cities and towns contributes to subsidence in the Bogotá savanna. The construction of new multifamily buildings, factories, warehouses, and other structures has resulted in structural load consolidation in the soil, as captured by radar, which can persist for up to 20 years or more.
- However, the absence of current and publicly accessible data on piezometric levels or water table levels in the area presents challenges for research. A public and comprehensive information system should be established to facilitate future studies on underground water usage and piezometric monitoring systems. The MT-InSAR analysis plays a crucial role in an early warning system that identifies areas requiring monitoring and intervention for subsidence-related issues. Nevertheless, the system can be complemented by other geodetic monitoring systems.

Author Contributions: Conceptualization, J.S.T.D., A.M.R.-A. and J.J.S.; methodology, J.S.T.D., A.M.R.-A. and J.J.S.; software, J.S.T.D., A.M.R.-A. and J.J.S.; validation, J.S.T.D., A.M.R.-A., J.J.S., G.E.Á.Á. and G.M.; formal analysis, J.S.T.D., A.M.R.-A., J.J.S., G.E.Á.Á. and G.M.; investigation, J.S.T.D., A.M.R.-A., J.J.S., G.E.Á.Á. and G.M.; resources, J.S.T.D., A.M.R.-A. and J.J.S.; writing—original draft preparation, J.S.T.D., A.M.R.-A. and J.J.S.; writing—review and editing, J.S.T.D., A.M.R.-A., J.J.S., G.E.Á.Á. and G.M.; visualization, J.S.T.D., A.M.R.-A., J.J.S., G.E.Á.Á. and G.M.; supervision, J.S.T.D., A.M.R.-A., J.J.S., G.E.Á.Á. and G.M.; funding acquisition, A.M.R.-A. All authors have read and agreed to the published version of the manuscript.

Funding: The APC was funded by University of Jaén (Spain).

Data Availability Statement: Not applicable.

Acknowledgments: Sentinel–1A/B data were freely provided by ESA through the Copernicus Programme. Data have been processed by SARPROZ (Copyright, 2009–2023, Daniele Perissin). The satellite orbits are from the ESA Quality control Group of Sentinel–1. Research was supported by (a) SIAGUA project PID2021–128123OB–C21 and PID2021–128123OB–C2, funded by MCIN/AEI/10.13039/501100011033/FEDER, UE); (b) POAIUJA–2023/2024 and CEACTEMA from University of Jaén (Spain); and (c) the RNM–282 research group from the Junta de Andalucía (Spain).

Conflicts of Interest: The authors declare no conflict of interest.

References

1. Foroughnia, F.; Nemati, S.; Maghsoudi, Y.; Perissin, D. An Iterative PS-InSAR Method for the Analysis of Large Spatio-Temporal Baseline Data Stacks for Land Subsidence Estimation. *Int. J. Appl. Earth Obs. Geoinf.* **2019**, *74*, 248–258. [CrossRef]
2. Galloway, D.; Jones, D.R.; Ingebritsen, S.E. *Land Subsidence in the United States*; USGS: Reston, VA, USA, 1999. [CrossRef]
3. De Vallejo, L.I.G.; Ferrer, M.; Ortuño, L.; Oteo, C. *Ingeniería Geológica*, 1st ed.; Alhambra, Ed.; Pearson Educación: London, UK, 2002.
4. Figueroa-Miranda, S.; Tuxpan-Vargas, J.; Ramos-Leal, J.A.; Hernández-Madrigal, V.M.; Villaseñor-Reyes, C.I. Land Subsidence by Groundwater Over-Exploitation from Aquifers in Tectonic Valleys of Central Mexico: A Review. *Eng. Geol.* **2018**, *246*, 91–106. [CrossRef]
5. Neely, W.R.; Borsa, A.A.; Burney, J.A.; Levy, M.C.; Silverii, F.; Sneed, M. Characterization of Groundwater Recharge and Flow in California's San Joaquin Valley From InSAR-Observed Surface Deformation. *Water Resour. Res.* **2021**, *57*, e2020WR028451. [CrossRef] [PubMed]
6. Shi, X.; Wu, J.; Ye, S.; Zhang, Y.; Xue, Y.; Wei, Z.; Li, Q.; Yu, J. Regional Land Subsidence Simulation in Su-Xi-Chang Area and Shanghai City, China. *Eng. Geol.* **2008**, *100*, 27–42. [CrossRef]
7. He, X.C.; Yang, T.L.; Shen, S.L.; Xu, Y.S.; Arulrajah, A. Land Subsidence Control Zone and Policy for the Environmental Protection of Shanghai. *Int. J. Environ. Res. Public Health* **2019**, *16*, 2729. [CrossRef]
8. Sato, C.; Haga, M.; Nishino, J. Land Subsidence and Groundwater Management in Tokyo. *Int. Rev. Environ. Strateg.* **2006**, *6*, 403–424.
9. Ruiz-Constán, A.; Ruiz-Armenteros, A.M.; Martos-Rosillo, S.; Galindo-Zaldívar, J.; Lazecky, M.; García, M.; Sousa, J.J.; Sanz de Galdeano, C.; Delgado-Blasco, J.M.; Jiménez-Gavilán, P.; et al. SAR Interferometry Monitoring of Subsidence in a Detritic Basin Related to Water Depletion in the Underlying Confined Carbonate Aquifer (Torremolinos, Southern Spain). *Sci. Total Environ.* **2018**, *636*, 670–687. [CrossRef]
10. Hu, L.; Navarro-Hernández, M.I.; Liu, X.; Tomás, R.; Tang, X.; Bru, G.; Ezquerro, P.; Zhang, Q. Analysis of Regional Large-Gradient Land Subsidence in the Alto Guadalentín Basin (Spain) Using Open-Access Aerial LiDAR Datasets. *Remote Sens. Environ.* **2022**, *280*, 113218. [CrossRef]
11. Modoni, G.; Darini, G.; Spacagna, R.L.; Saroli, M.; Russo, G.; Croce, P. Spatial Analysis of Land Subsidence Induced by Groundwater Withdrawal. *Eng. Geol.* **2013**, *167*, 59–71. [CrossRef]
12. Poland, J.F. *Guidebook to Studies of Land Subsidence Due to Ground-Water Withdrawal*; UNESCO: London, UK, 1987; Volume 2. [CrossRef]
13. Sosa Ruiz, D.; López-Caloca, A.A.; Couturier, S. Posibilidades y Limitaciones de La Interferometría Radar (InSAR) Con Imágenes de Una y Dos Polarizaciones Para El Monitoreo de Áreas Urbanas. Caso de Estudio: Zona Metropolitana Del Valle de México. In *Análisis Geoespacial En Los Estud. Urbanos*; National Autonomous University of Mexico: Mecixo City, Mexico, 2018; pp. 15–38.
14. Farolfi, G.; Bianchini, S.; Casagli, N. Integration of GNSS and Satellite InSAR Data: Derivation of Fine-Scale Vertical Surface Motion Maps of Po Plain, Northern Apennines, and Southern Alps, Italy. *IEEE Trans. Geosci. Remote Sens.* **2019**, *57*, 319–328. [CrossRef]
15. Müller, M.D.; Geiger, A.; Kahle, H.G.; Veis, G.; Billiris, H.; Paradissis, D.; Felekis, S. Velocity and Deformation Fields in the North Aegean Domain, Greece, and Implications for Fault Kinematics, Derived from GPS Data 1993–2009. *Tectonophysics* **2013**, *597–598*, 34–49. [CrossRef]
16. Lazos, I.; Chatzipetros, A.; Pavlides, S.; Pikridas, C.; Bitharis, S. Tectonic Crustal Deformation of Corinth Gulf, Greece, Based on Primary Geodetic Data. *Acta Geodyn. Geomater.* **2020**, *17*, 413–424. [CrossRef]
17. Hollenstein, C.; Müller, M.D.; Geiger, A.; Kahle, H.G. Crustal Motion and Deformation in Greece from a Decade of GPS Measurements, 1993–2003. *Tectonophysics* **2008**, *449*, 17–40. [CrossRef]
18. Chalouan, A.; Gil, A.J.; Galindo-Zaldívar, J.; Ahmamou, M.; Ruano, P.; De Lacy, M.C.; Ruiz-Armenteros, A.M.; Benmakhlouf, M.; Riguzzi, F. Active Faulting in the Frontal Rif Cordillera (Fes Region, Morocco): Constraints from GPS Data. *J. Geodyn.* **2014**, *77*, 110–122. [CrossRef]
19. Sanchez, L.; Martínez, W.; Herrera, I.; Téllez, L. *Estimación de La Subsidencia En Bogotá a Partir de Mediciones GNSS y Nivelación Geométrica*; IGAC: Montevideo, Uruguay, 2008.
20. Blanco, P.; Barreto, G.; Ortiz Abaunza, D. *La Interferometría Diferencial Dinsar—Una Técnica para el Monitoreo de la Subsidencia en Bogotá d.C*; Department of Prevention and Emergency of the District of Bogotá: Bogotá, Colombia, 2009; pp. 1–15.

21. Ávila, G.; Castro Villamarín, N. Avances En El Estudio de Subsidencia En La Ciudad de Bogotá. In Proceedings of the VIII International Conference on Geotechnical Engineering, Colombo, Sri Lanka, 6 December 2011; pp. 6-1–6-11.
22. Mora Paéz, H.; Díaz Mila, F.; Cardona, L. Mapping Land Subsidence in Bogotá, Colombia, Using the Interferometric Synthetic Aperture Radar (InSAR) Technique with TerraSAR–X Images. *His Master's Voice* **2020**, *4*, 515–548. [CrossRef]
23. Landscapes, W.G. *Landscapes and Landforms of Colombia*; Hermelin, M., Ed.; World Geomorphological Landscapes; Springer International Publishing: Cham, Switzerland, 2016. [CrossRef]
24. Lobo-Guerrero, A.; Gilboa, Y. Grounwater in Colombia. *Hydrol. Sci. J.* **1987**, *32*, 161–178. [CrossRef]
25. Montoya Arenas, D.M.; Reyes Torres, G.A. *Geología de La Sabana de Bogotá. Instituto Colombiano de Geología y Minería (INGEOMINAS)*; Instituto Colombiano de Geología y Minería (INGEOMINAS): Bogotá, Colombia, 2005; p. 105.
26. Lobo-Guerrero, A. *Geología e Hidrogeología de Santafé de Bogotá y Su Sabana*; Columbian Society of Geothechnology: Bogotá, Colombia, 1992.
27. Lobo-Guerrero, A. Descenso de Niveles de Agua Subterránea En La Sabana de Bogotá. In Proceedings of the VIII Jornadas Geotécnicas de la Ingineria en Colombia-II Foro Sobre Geotecnica de la Sabana Bogotá, Bogotá, Colombia, 8–10 December 1995; pp. 1–11.
28. Sabana Centro Cómo Vamos. Análisis de la Situación Poblacional Sabana Centro; Bogotá. 2018. Available online: https://sabanacentrocomovamos.org/home/wp-content/uploads/2019/11/Informe-An%C3%A1lisis-de-la-situaci%C3%B3n-poblacional-de-Sabana-Centro.pdf (accessed on 1 October 2023).
29. Córdoba Álvarez, R.D. *Una Aproximación Estocástica Para Modelar y Caracterizar los Episodios Torrenciales en el Espacio y el Tiempo—Caso de Estudio Sabana de Bogotá*; Universidad de los Andes: Bogotá, Colombia, 2012.
30. Corporación Autónoma Regional de Cundinamarca, C. *Plan de Manejo Ambiental de Agua Subterránea En La Sabana de Bogotá y Zona Critica*, 1st ed.; Imprenta Nacional de Colombia: Bogotá, Colombia, 2019; p. 176.
31. Tomas, R.; Herrera, G.; José, D.; Peña, F. Subsidencia Del Terreno. *Enseñanza Cienc.* **2009**, *17*, 295–302.
32. Ojeda, J.; Donnelly, L. Landslides in Colombia and Their Impact on Towns and Cities. *Remote Sens.* **2006**, *112*, 103–122.
33. Ingeominas; Universidad de los Andes. Microzonificacion Sismica de Santa Fe de Bogotá.Convenio Interadministrativo 01-93.Pdf; Santa. Available online: https://www2.sgc.gov.co/biblioteca/Documents/Biblioteca/Microzonificacion%20sismica%20de%20santa%20fe%20de%20bogota.pdf (accessed on 1 October 2023).
34. Lizarazo, P. *La Integración de La Región Capital Hacia 2038*; Subdirección Imprenta Distrital DDD: Bogotá, Colombia, 2011.
35. Alfonso Piña, W.H.; Pardo Martínez, C.I. Urban Material Flow Analysis: An Approach for Bogotá, Colombia. *Ecol. Indic.* **2014**, *42*, 32–42. [CrossRef]
36. López Hernández, C.N.; Jaramillo Garcés, M.M.; Avendaño, A.J.; Pérez Otavo, D.; Romero, Y.E.; Gaitán Victoria, C.E. *Indicadores de Consumo de Agua y Energia Eléctrica*; Alcaldia Mayor de Bogotá, Secretaria de Planeación: Bogotá, Colombia, 2020.
37. Ávila, G. *Estudio de La Retracción y El Agrietamiento de Arcillas. Aplicación a La Arcilla de Bogotá*; Universitat Politècnica de Catalunya: Barcelona, Spain, 2004.
38. Fárová, K.; Jelének, J.; Kopačková-Strnadová, V.; Kycl, P. Comparing DInSAR and PSI Techniques Employed to Sentinel_1 Data to Monitor Highway Stability_ A Case Study of a Massive Dobkovičky Landslide_Czech Republic.Pdf. *Remote Sens.* **2019**, *11*, 2670. [CrossRef]
39. Zhong, L.; Jixian, Z.; Yonghong, Z.; Dzurisin, D. Monitoring and Characterizing Natural Hazards with Satellite InSAR Imagery. *Ann. GIS* **2010**, *16*, 55–66. [CrossRef]
40. Perissin, D. Interferometric SAR Multitemporal Processing: Techniques and Applications. *Remote Sens. Digit. Image Process.* **2016**, *20*, 145–176. [CrossRef]
41. Ferretti, A.; Prati, C.; Rocca, F. Permanent Scatterers in SAR Interferometry. *IEEE Trans. Geosci. Remote Sens.* **2001**, *39*, 8–20. [CrossRef]
42. Mora, O.; Lanari, R.; Mallorqui, J.J.; Berardino, P.; Sansosti, E. A New Algorithm for Monitoring Localized Deformation Phenomena Based on Small Baseline Differential SAR Interferograms. In Proceedings of the IEEE International Geoscience and Remote Sensing Symposium, Toronto, ON, Canada, 24–28 June 2002; Volume 2, pp. 1237–1239. [CrossRef]
43. Hooper, A.J. A Multi-Temporal InSAR Method Incorporating Both Persistent Scatterer and Small Baseline Approaches. *Geophys. Res. Lett.* **2008**, *35*, 1–5. [CrossRef]
44. Crosetto, M.; Monserrat, O.; Cuevas-González, M.; Devanthéry, N.; Crippa, B. Persistent Scatterer Interferometry: A Review. *ISPRS J. Photogramm. Remote Sens.* **2016**, *115*, 78–89. [CrossRef]
45. Hooper, A.; Bekaert, D.; Spaans, K.; Arikan, M. Recent Advances in SAR Interferometry Time Series Analysis for Measuring Crustal Deformation. *Tectonophysics* **2012**, *514–517*, 1–13. [CrossRef]
46. Beladam, O.; Balz, T.; Mohamadi, B.; Abdalhak, M. Using Ps-Insar with Sentinel-1 Images for Deformation Monitoring in Northeast Algeria. *Geosciences* **2019**, *9*, 315. [CrossRef]
47. IGAC. Red MAGNA ECO. Available online: https://www.igac.gov.co/es/contenido/areas-estrategicas/red-magna-eco (accessed on 1 October 2023).
48. IGAC. MAGNA-SIRGAS. Available online: https://www.igac.gov.co/es/contenido/areas-estrategicas/magna-sirgas (accessed on 1 October 2023).
49. SIRGAS. SIRGAS: Sobre Nosotros. Available online: https://www.sirgas.org/es/sirgas-definition/ (accessed on 1 October 2023).

50. Sánchez, L.; Drewes, H.; Brunini, C.; Mackern, M.V.; Martínez-Díaz, W. *SIRGAS Core Network Stability*; Springer: Cham, Switzerland, 2015; pp. 183–191. [CrossRef]
51. Sánchez, L.; Drewes, H. Crustal Deformation and Surface Kinematics after the 2010 Earthquakes in Latin America. *J. Geodyn.* **2016**, *102*, 1–23. [CrossRef]
52. Sánchez, L.; Drewes, H. Geodetic Monitoring of the Variable Surface Deformation in Latin America. In *Beyond 100: The Next Century in Geodesy, Proceedings of the IAG General Assembly, Montreal, QC, Canada, 8–18 July 2019*; Springer International Publishing: Cham, Switzerland, 2020. [CrossRef]
53. Escobar Castro, G.; Marantes González, L.E.; Lindon Losada, G.P.; Díaz Parra, F.J. Zonificación de la Respuesta Sísmica de Bogotá para el Diseño Sismo Resistente de Edificaciones; Bogotá. D.C. 2010. Available online: https://www.idiger.gov.co/documents/20182/112614/Zonificacion_Respuesta_Sismica-FOPAE-2010.pdf (accessed on 1 October 2023).
54. Kaniuth, K.; HäfeleHafele, P.; Sánchez, L. Subsidence of the Permanent GPS Station Bogotá. In *Vertical Reference Systems. International Association of Geodesy Symposia, vol 124.*; Drewes, H., Dodson, A.H., Fortes, L.P.S., Sánchez, L., Sandoval, P., Eds.; Springer: Berlin/Heidelberg, Germany, 2002; pp. 56–59. [CrossRef]
55. Rudenko, S.; Schön, N.; Uhlemann, M.; Gendt, G. Reprocessed Height Time Series for GPS Stations. *Solid Earth* **2013**, *4*, 23–41. [CrossRef]
56. Mora–Páez, H.; Kellogg, J.N.; Freymueller, J.T. Contributions of Space Geodesy for Geodynamic Studies in Colombia: 1988 to 2017. In *LR Lloyd's Register*; Gómez, J., Pinilla–Pachon, A.O., Eds.; Servicio Geológico Colombiano: Bogotá, Colombia, 2019; Volume 100, pp. 479–498. [CrossRef]
57. Lobo-Guerrero, A. Effects of Aquifer Overexploitation on the Surface Infrastructure in the Bogotá Sabana (Colombia). *RMZ-Mater. Geoenviron.* **2003**, *50*, 193–196.

Disclaimer/Publisher's Note: The statements, opinions and data contained in all publications are solely those of the individual author(s) and contributor(s) and not of MDPI and/or the editor(s). MDPI and/or the editor(s) disclaim responsibility for any injury to people or property resulting from any ideas, methods, instructions or products referred to in the content.